Australia's National
Science Agency

UltraFine+® Next Gen Analytics

Geological Survey of Queensland – Jericho Project

Anicia Henne, Ryan RP Noble, Fang Huang, Dave Cole, Morgan Williams, Ian C Lau, Tania Ibrahimi

EP2023-0486
March 2023

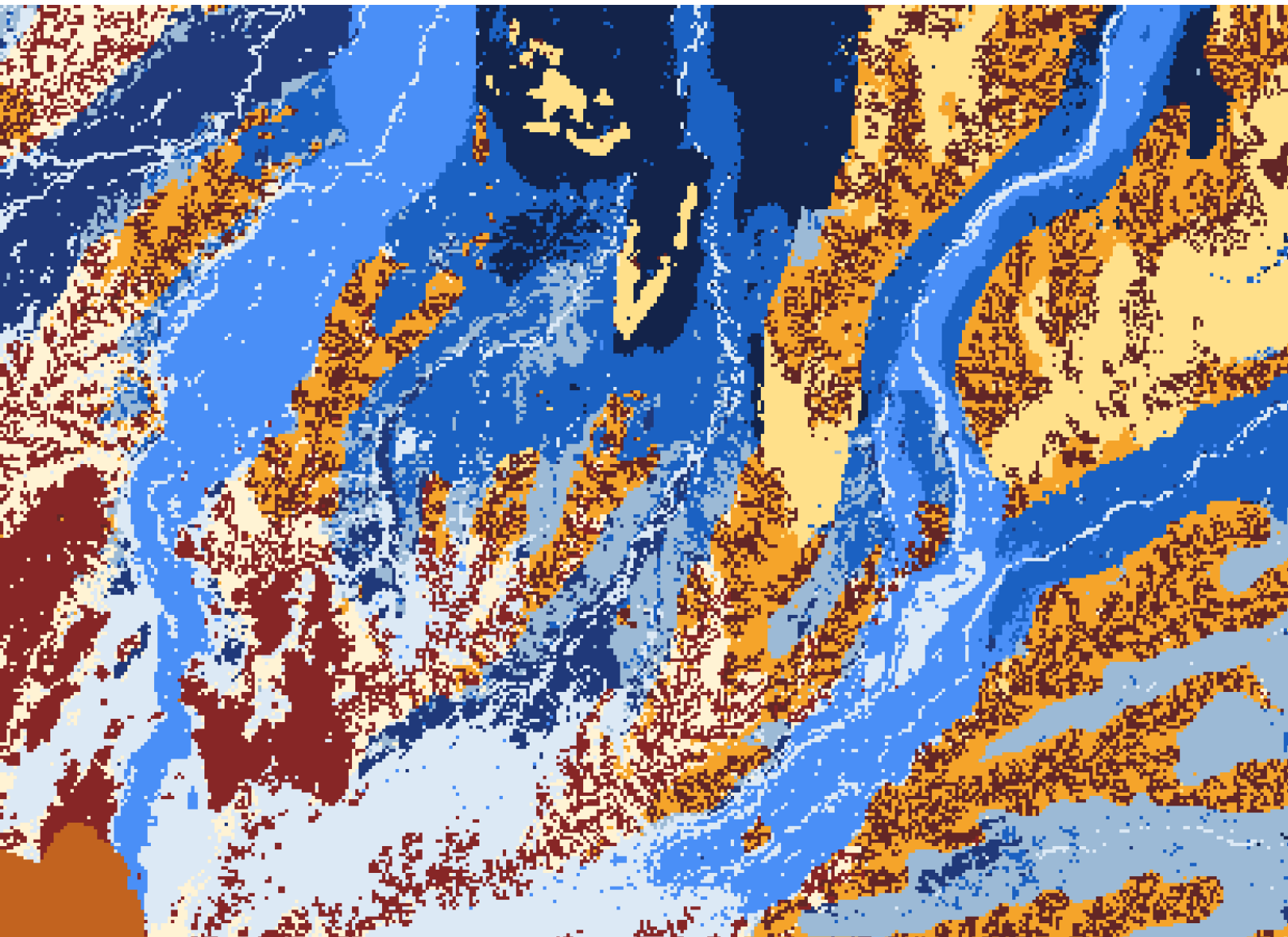

Citation

Henne A, Noble RRP, Huang F, Cole D, Williams M, Lau IC, Ibrahimi T (2023). UltraFine+® Next Gen Analytics. Geological Survey of Queensland – Jericho. CSIRO Report EP2023-0486, CSIRO, Australia.

Copyright

Important disclaimer

UltraFine+® Next Gen Analytics Sponsors

UltraFine+® Next Gen Analytics for Discovery

The Geological Survey of Queensland (GSQ) contributed samples collected by Minotaur Exploration over the prospective Jericho project site to the UltraFine+® Next Gen Analytics research project conducted by CSIRO in collaboration with LabWest and over 20 industry sponsors and state and territory geological surveys. The aim of the broader UltraFine+® Next Gen Analytics for Discovery research project is to facilitate a paradigm shift for precious, base, and critical metals exploration in Australia by combining UltraFine+® soil analytical methods with purpose-built data integration tools, adding value to routine soil sampling in frontline exploration and shaping mineral exploration approaches for the coming decades.

It has been common practice to use soil geochemistry in mineral exploration with little regard for physicochemical soil parameters or landform settings, and how these relate to buried mineralisation. The UltraFine+® Next Gen Analytics research addresses this challenge by delivering an analytical refinement of the UltraFine+® soil analysis method and by adding relevant mineral proxies via spectral mineralogy and the soil properties pH, EC and particle size distribution to the workflow and interpretation. UltraFine+® Next Gen Analytics utilises machine learning to integrate these soil parameters with regolith landscape models. This improves our ability to identify targets and false positives, as well as understand the spatial variance and influence of regolith types. With the development of a robust set of measurable parameters and new data products to fully assess underappreciated soil properties, the UltraFine+® Next Gen Analytics data package provides the next generation analytical tools for mineral explorers to make qualified decisions on when and where to direct further exploration.

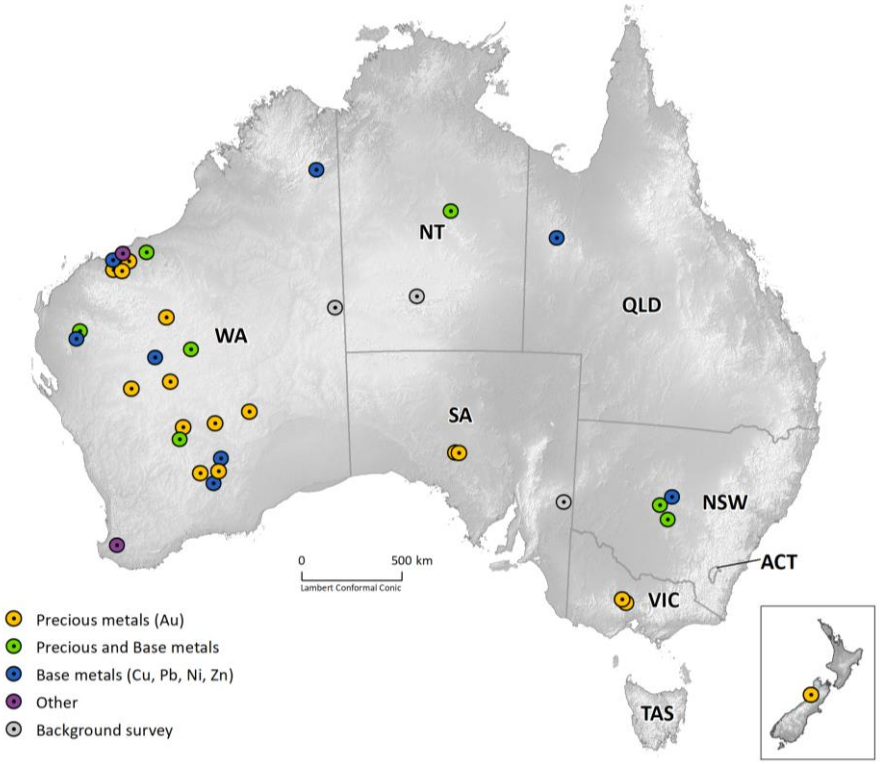

Figure 1: UltraFine+® Next Gen Analytics for Discovery project sponsors' site locations (as of 1 February 2023).

Contents

Figures

Tables

Acknowledgments

This project received financial support from many government and industry bodies. Financial supporters include the Minerals Research Institute of Western Australia, Geological Survey of Queensland, Geological Survey of South Australia, Geological Survey of New South Wales, Northern Territory Geological Survey, Geological Survey of Western Australia, Kalamazoo Resources, MCA Nominees, Iceni Gold, Siren Gold, Dreadnought Resources, De Grey Mining, Carnavale Resources, Fortescue Metals Group, Newmont, Northern Star Resources, Kairos Minerals, Emmerson Resources, Independence Group, Western Gold Resources, Capricorn Metals, Hexagon Energy Materials, Monger Gold, Strategic Energy Resources, Barton Gold, Ozz Resources, Anax Metals and Lodestar Minerals. In-kind support for the project was provided by CSIRO and LabWest.

Most critically, we thank the above contributors for their in-kind support in providing UltraFine+® analytical results from many, many soils across Australia. This support totalled several millions of dollars and without the large number of results the outcomes of this project would have been severely limited.

In addition to the above industry sponsors, Minotaur Exploration (now part of AIC Mines via Andromeda Metals and Demetallica Limited) provided the Geological Survey of Queensland (GSQ) with the soils sampled from the Jericho site for this project. AIC provided outlines of the main mineralisation lodes. Sample collection was provided in-kind by Minotaur Exploration and analyses for the project area were funded by the GSQ.

Executive summary

The Geological Survey of Queensland submitted 69 “blind” soil samples (without previous context) over the Jericho deposit south-east of Cloncurry in northwest Queensland as part of the UltraFine+® Next Gen Analytics research project. The broader UltraFine+® Next Gen Analytics research project consists of three main components:

a) refining the UltraFine+® soil analytical method designed to extract mobile element signatures from the ultrafine fraction (<2 µm) of a given sample by lowering detection limits and adding additional soil properties (pH, electrical conductivity, soil sizing and spectral mineralogy) to the standard soil analysis;

b) developing the Next Gen Analytics workflow using machine learning to create landscape context from spatial data features for soil geochemical interpretation; and

c) providing a comprehensive data package to project sponsors.

Assessing geochemical data in mineral exploration often focuses on understanding outliers, such as elevated copper, gold, or zinc. Often the largest concentrations are followed up, but landscape and soil types can significantly influence concentration. For example, high metal concentrations may be readily identifiable as outliers in a geochemical dataset where samples were collected over mineralisation in areas of shallow residual soils, while the same mineralisation has a much weaker elemental signal in samples collected over thicker depositional landscapes. With the ability to approximate landscape types from spatial data features via machine learning, the UltraFine+® Next Gen Analytics workflow was developed to improve outlier identification within each landscape type.

The UltraFine+® Next Gen Analytics data package includes maps of machine learning derived landscape clusters, maps, and boxplots of elemental outliers by landscape type, exploration indices for rapid, first-pass identification of element associations, dispersion and source directions, soil texture diagrams, as well as automated QAQC of geochemistry, VNIR (visible to near-infrared) spectral mineralogy, particle size distribution and pH and EC (electrical conductivity). This data is also available on maps and as CSV and shapefiles. This provides a basic, first-pass interpretation of geochemical samples by proxy regolith type and the identification of otherwise “overlooked or subtle” potential anomalies of interest to mineral exploration.

The Jericho project site constitutes the smallest project area of the more than 40 sites that are part of the UltraFine+® Next Gen Analytics research project. The site was part of the earliest developments to assess the effectiveness of the UltraFine+® method, to test the principal functionality of the Next Gen Analytics workflow, and to conduct first-pass testing of the outputs over areas with tangible exploration targets. The data presented herein was analysed in August 2019. Since then, the components of the workflow have undergone continuous improvements, especially with regards to the consistency of pH and VNIR measurements, as well as the addition of soil particle size analysis, Fourier transform infrared spectroscopy (FTIR) and Pd analyses. The Jericho data were essential in developing these improvements.

The UltraFine+® method is well suited to leverage existing dispersion mechanisms during weathering in shallow transported cover. However, exploration settings with mineralisation at depths of >30 m below transported cover, and/or without dispersion mechanisms in place will not be conducive to surface geochemical sampling (including the UltraFine+® approach). Regrettably, the depth to mineralisation (>200 m), small area size (3 km^2), poor landscape diversity (exclusively depositional landscape settings), as well as the low number of samples per landscape type which did not extend into assumed geochemical background, limited the utility of the UltraFine+ ® Next Gen Analytics outputs at the Jericho site. Hence, it is recommended to interpret the geochemical results as a whole dataset rather than by landscape type.

Maximum concentrations of the main metals of interest were measured at 0.26 ppm for Ag, 16.5 ppb for Au, and 55.3 ppm for Cu, against median values of 0.05 ppm Ag, 3.3 ppb Au, and 38.7 ppm Cu. No analysis for these elements was below the detection limit. However, there was generally insufficient data (in terms of number of samples and spatial extent) to identify lateral background soil concentrations and/or information on dispersion mechanisms from depth to surface. Hence, these subtle, elevated concentrations are likely to be entirely coincidental. Individual outliers not apparent from the whole-population analyses were identified by landscape types for exploration relevant elements such as Cd, Co, Cr, Mo, Pb, Sb and W, but these did not exhibit discernible patterns.

A variety of clustering methods were trialled during the development of the Next Gen Analytics workflow to generate appropriate proxies for regolith types and here we present only the final outputs run in November 2022. All outputs presented in this report provide a more detailed landscape context than publicly available regolith products. The recommended outputs for the Jericho project area are those produced via a *k*-means algorithm with four landscape clusters (kmeans4). Since the small area size with exclusively depositional landscape settings, as well as the number of soil samples per landscape cluster limited the interpretation within landscape context, we demonstrate an additional example of the machine learned landscape clustering approach for future greenfield exploration surveys in Queensland. In this example we generated a larger area proxy landscape map (approximately 1,600 km^2) centred around the Jericho project area with twelve landscape clusters. This proxy landscape map successfully identifies the major landscape types in residual, erosional and depositional settings and provides a much more in-depth landscape context than publicly available maps and could aid soil sample survey design as well as data interpretation.

With the limited samples and context available, principal component analysis, regolith ratios and indices, as well as other soil property analyses, reflect landscape variety within the dataset rather than relevant exploration criteria. As such, they were of use differentiating similar materials in the north and south of the project site and thereby confirmed the validity of the landscape model. The additional soil property data shows some interesting trends with links to the machine learning derived landscape types within the area.

1 The UltraFine+® Next Generation Analytics for Discovery Research Project

Much of Australia's remaining potential mineral wealth is masked by regolith cover that poses a challenge for future mineral exploration, especially in transported cover. The mobile element signature of interest for exploration in these materials is commonly contained in the < 2 µm "ultrafine" particle size fraction (Noble et al. 2020). This is likely due to the presence of "scavenging phases" such as clays, organic compounds and various oxides/oxyhydroxides that dominate this fine fraction (Hall 1998). The CSIRO in collaboration with LabWest developed the novel UltraFine+® method, which is optimised for multi-element analysis of this ultrafine soil fraction. This improved soil geochemistry workflow generates results with more contrast and increased concentrations of Au, Cu and Zn, and removes the nugget effect, thereby enhancing the reproducibility and reliability of results (Noble et al. 2020).

The UltraFine+® Next Gen Analytics research project leverages and expands on this workflow by adding relevant soil parameters including spectral mineral proxies, pH, Electrical Conductivity (EC), and particle size distribution to the UltraFine+® method as standard analyses. This provides a wealth of additional data to the standard soil sample exploration package, which enables exploration geologists to investigate the relationships between soil geochemistry and other physicochemical soil parameters and their relationship to buried mineralisation. In addition, the UltraFine+® Next Gen Analytics workflow utilises machine learning approaches to produce landscape context for, and first-pass data interpretation of, these soil sample analyses.

1.1 Geological Survey of Queensland – Jericho project

The Geological Survey of Queensland (GSQ) submitted 69 soil samples from five transects over the Jericho deposit as part of the UltraFine+® Next Gen Analytics project (Figure 2). The Jericho Cu-Au deposit is located approximately 65 km south-east of Cloncurry in northwest Queensland, and 4 km south of the Eloise copper-gold mine (Figure 2). The Jericho project site covers an area of approximately 3 km^2 within Demetallica's Chimera Project tenement package and is prospective for copper, gold and silver. In their most recent mineral resource estimate from October 2022, Demetallica estimates a total indicated and inferred resource of 14.1 million tonnes at 1.46% Cu, 0.29 g/t Au and 1.6 g/t Ag, with a 0.85% Cu cut-off (Demetallica 2022). Demetallica was recently acquired by AIC Mines Ltd.

Copper at the Jericho deposit is hosted in two lodes (J1 and J2) associated with massive to semi-massive chalcopyrite and pyrrhotite with minor pyrite and arsenopyrite mainly associated with quartz veins in discrete, steeply dipping (70 – 75˚ to the west) biotite-rich shear zones. The two lodes run parallel from south to north, with approximately 120 m between lodes (https://demetallica.com.au/projects/jericho/; Minotaur Exploration Limited 2019). The mineral assemblage, texture and geochemistry, as well as host rocks at Jericho have been reported as very similar to the nearby Eloise deposit (Minotaur Exploration Limited 2019).

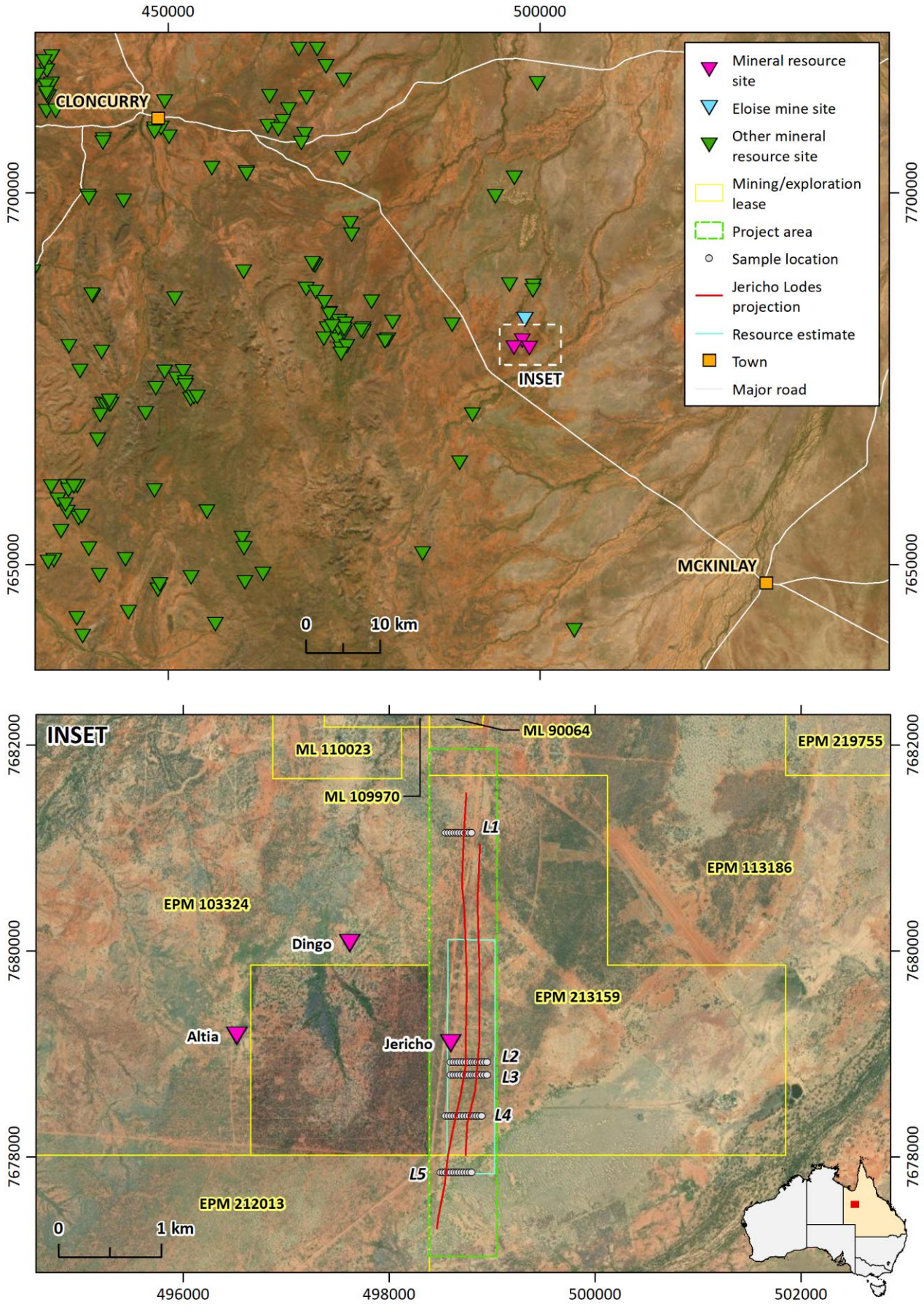

Figure 2: General location of the Jericho project area near Cloncurry in QLD. Inset shows tenement boundaries, modelled project area and main prospects. L1 to L5 refer to the soil sample transects.

The mineralisation, regolith landform, and material around the Eloise deposit has been described by various authors (summarised in Anand 2016 from Baker 1994, Li Shu and Robertson 1997, and Anand and Robertson 2012). The general regolith landform containing both the Eloise and Jericho deposits is dominated by undulating to rolling plains. The Proterozoic basement rocks that host the ore-bearing shears, are truncated by an unconformity overlain by Mesozoic mudstone (Li Shu and Robertson 1997) which in turn is covered by thick (50 m to 70 m; Anand 2016) transported Tertiary and Quaternary fluvial sediments.

The regolith within the immediate Jericho project area is dominated by sand or gravel plains with some influence of deeply weathered ferricrete-cemented alluvium that appears as residuum in the landforms (inverted relief). Quartz dominated sand in the north and south commonly contain ferruginous pisoliths or pebbles, or other mixed cemented materials such as localised clay, calcrete, laterite, silcrete, silt and colluvium. The very south of the project area is the edge of a broad alluvial flood plain that is draining towards the Fullarton River (Figure 3).

Three major soil types are noted in the Jericho project area. These are the distinct soil orders Kandosols, Sodosols, and Dermosols or KO, SO and DE types, respectively (Australian Soil Classification System; Isbell 2012). The central section of the project area is dominated by kandosols (KO type). These soils lack strong texture contrast and have little structure in B horizons without significant calcareous material. Theses soils have a field texture of sand, loamy sand, or clayey sand as well as <15 % clay horizons (i.e., they do not exhibit strong soil clay increases with depth) and are common throughout inland Queensland. Sodosols (SO type), which usually display a clay increase in the B horizon, a higher pH, and are commonly associated with salts, dominate the southern edge of the project area. The northern extent of the area is dominated by Dermosols (DE type) which also have structured B horizons (commonly a clay increase) but lack the differentiation or strong texture-contrast between the surface (A) horizon and lower (B) horizons. These soils tend to have a larger clay fraction in arid regions compared to the other soil types in the project area.

The Jericho project area is dominated by grassland with hot, dry summers and mild winters, an average annual rainfall of 483.1 mm and an average annual evapotranspiration rate between 400 to 500 mm/year. The mean minimum and maximum temperatures are 18.5 and 32.2°C, respectively (Bureau of Meteorology 2023).

The Geological Survey of Queensland submitted “blind” samples (without previous context) to the UltraFine+® Next Gen project to test the approach of the UltraFine+® soil analytical method. However, considering the thickness of sedimentary cover, the depth of mineralised intercepts in basement rocks (several hundred metres), and little-preserved weathering near the unconformity, it is unlikely for any soil geochemical sampling to identify element dispersion related to the mineralisation at depth. In addition, sample transects are located within the current resource footprint across the two lodes and do not extend into assumed geochemical background (Figure 2).

The Next Gen Analytics workflow was designed primarily for greenfield exploration areas in transported cover with 100s to 1000s of soil samples and to generate interpretation of these samples prior to significant ground disturbance (e.g., major roads, built-up areas, and mining and agricultural infrastructure) as this can influence multi-spectral images used in this workflow. The small number of samples and ground disturbance over the Jericho project area limit the value of

interpreting samples by landscape type for this specific site and some of the analyses, which are now part of the standard UltraFine+® suite (e.g., Br, I, Pd, FTIR) were not yet developed when this data was analysed. However, we have used this site, along with other early supporters of the project, to develop the UltraFine+® Next Gen Analytics workflow and present in this report the various outputs as a brief demonstration. Since this project site constitutes the smallest project area of the more than 40 sites that were modelled during the Next Gen research project, the focus for this project site was on principal functionality and application of landscape recognition via machine learning in a known exploration setting and testing its limitations.

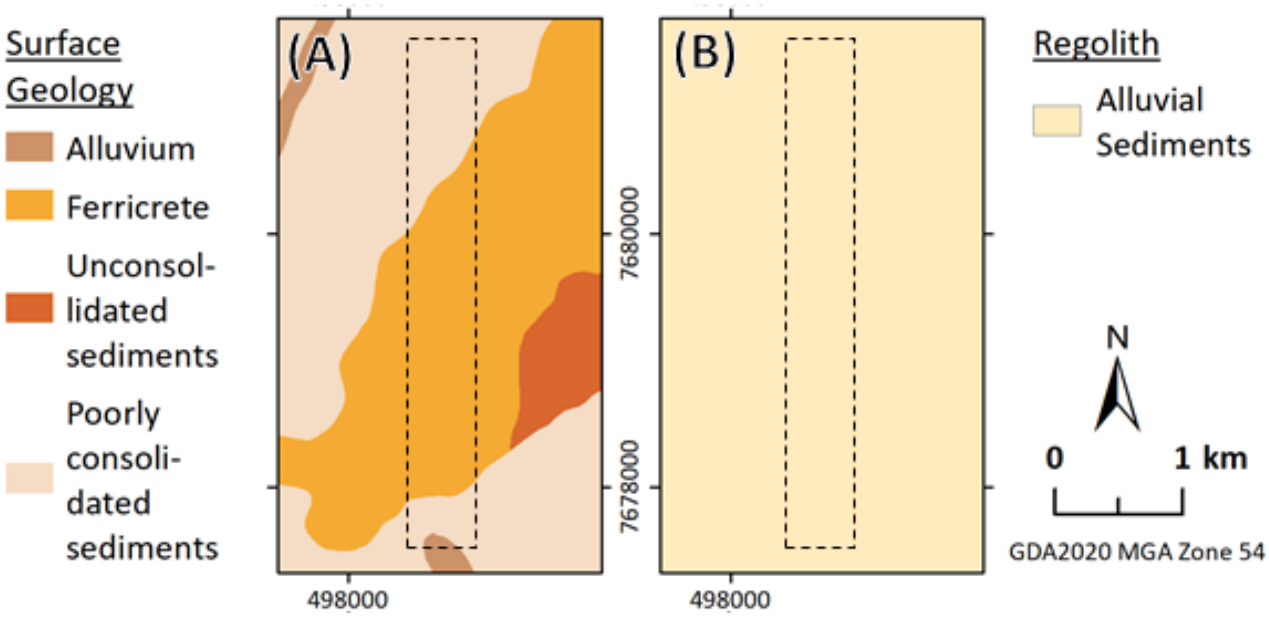

Figure 3: Surface (Department of Resources 2018) and regolith geology (Geoscience Australia 2013) in the Jericho project area. Dashed boxes indicate the extent of the modelled area.

2 The UltraFine+® Next Gen Analytics Workflow

The UltraFine+® Next Gen Analytics workflow is based on the UltraFine+® soil sampling method previously developed by the CSIRO in collaboration with LabWest (Noble et al. 2020). In addition to further improving the UltraFine+® method by lowering detection limits and adding valuable soil properties, such as spectral mineralogy, to the standard analysis, the focus of the UltraFine+® Next Gen Analytics project is to provide landscape context for the geochemical data acquired, and a basic, first-pass data interpretation by incorporating semi-automated machine learning into the workflow. While the data for the Jericho project presented herein were analysed in August 2019 when some analyses (e.g., FTIR) were not yet available, the UltraFine+® Next Gen Analytics outputs presented in this report were re-processed in November 2022 upon finalisation of the Next Gen workflow.

2.1 Sample collection

Soil samples for the Jericho project area were collected prior to 2019 by Minotaur Resources from a 10 cm to 20 cm horizon for each sample. Samples were stored and dried in calico bags. Once dry, 2 kg of bulk soil sample material was passed through a 5 mm plastic sieve into a plastic collection bowl, and then hand-mixed to nominally homogenise. Sub-samples (approximately 200 g) were extracted from the primary collection bowl using a clean plastic trowel, placed in labelled paper bags and sent to LabWest in Perth. Analyses of 69 samples (Laboratory Job ALW004867) were received by CSIRO. These sample results were located along 5 transects crossing the Jericho lodes (J1 and J2; Figure 2). Transect 1 lies to the north of the current resource estimate area, while Transect 5 was sampled along the southern edge of the resource model area (Figure 2).

2.2 UltraFine+® laboratory soil analyses

All soil samples were analysed using the UltraFine+® method (Noble et al. 2020) at LabWest Pty Ltd, Perth, Australia. The complete workflow requires <40 g of soil and includes particle size distribution analysis, pH and EC measurements, separation of the ultrafine (<2 µm) size fraction, multi-elemental analyses, and spectral reflectance mineralogy. The components of the UltraFine+® workflow are undergoing continuous improvements over the course of the UltraFine+® Next Gen Analytics research project (conducted from April 2020 to April 2023) which is reflected in improved detection limits and refined outputs over time. The data presented herein was analysed in August 2019 and FTIR data was not collected.

2.2.1 Bulk soil properties

Electrical conductivity (EC) and pH were measured on bulk sample slurries using a TPS AQUA-CP/A meter. Slurries were prepared using de-ionised water with a 1:5 w/w soil-to-water ratio.

2.2.2 Soil sizing analysis

Particle size analyses were conducted on the bulk sample and measured using a Malvern Mastersizer 2000 in suspension.

2.2.3 UltraFine+® fine fraction separation

The ultrafine fraction (<2 µm; clay fraction) was extracted from each bulk sample via suspension in de-ionised water, addition of a dispersant and subsequent centrifugation and drying (Noble et al. 2020).

2.2.4 UltraFine+® extraction

The ultrafine fraction (<2 µm) of all soil samples was processed using a microwave-assisted aqua regia digestion (LabWest MAR-04) at LabWest Pty Ltd, Perth, Australia. The extractions were analysed for a suite of elements (Table 1) using ICP-OES (Perkin Elmer Optima 7300DV) and ICP-MS (Perkin Elmer Nexion 300Q). The microwave-assisted aqua regia digestion uses 0.2 - 0.4 g of soil with a 100 % mixture of 3:1 concentrated HCl:HNO_3. Unlike conventional extraction methods, the material is heated in a closed Teflon tube in an Anton Paar Multiwave PRO Microwave Reaction System for increased metal recovery (Noble et al. 2020).

Table 1: Number of samples analysed with the UltraFine+® workflow for GSQ's Minotaur project. *Added to the workflow after project data acquisition. †Analyses via ICP-OES.

ANALYSES	NUMBER OF SAMPLES	OUTPUTS
Microwave-assisted aqua regia on ultrafine fraction (LabWest MAR-04)	69	Ag, Al†, As, Au, Ba†, Be, Bi, Br*, Ca†, Cd, Ce, Co, Cr†, Cs, Cu, Fe†, Ga, Ge, Hf, Hg, I*, In, K†, La, Li†, Mg†, Mn†, Mo, Nb, Ni, Pb, Pd*, Pt, Rb, Re, S†, Sb, Sc†, Se, Sn, Sr†, Ta, Te, Th, Ti†, Tl, U, V†, W, Y, Zn, Zr
Bulk soil properties	69	EC, pH
Particle size distribution on bulk sample (LabWest SIZE-01)	69	Size fractions <2 µm, <50 µm, <125 µm, <250 µm, <1000 µm, <2000 µm, >2000 µm; d(0.1); d(0.5); d(0.9); specific surface area (SSA)
Visible-near-infrared (VNIR) on ultrafine fraction (LabWest NIR/SWIR)	69	Main minerals; kaolinite crystallinity; iron oxide species; relative abundance of iron oxide, kaolinite, white mica and aluminium smectite, iron substitution in kaolinite, chlorite and dark mica, iron and magnesium smectite, mafic minerals with OH; white mica and aluminium smectite composition; palygorskite; Munsell® colour; hue; saturation; intensity
Fourier transform infrared spectroscopy (FTIR) on ultrafine fraction (LabWest FTIR*)	0	Clay, quartz, and carbonate abundances; total organic carbon; gibbsite index

2.2.5 Visible near-infrared reflectance and short-wave infrared reflectance (VNIR-SWIR)

Visible near-infrared and short-wave infrared reflectance measurements were acquired on the ultrafine fraction (<2 µm) using a Spectral Evolution RS-3500 spectrometer (Serial Number

18980N3). The spectrometer measures electromagnetic radiation reflected off materials relative to that of a known reference material. The instrument collects spectra in the 350–2500 nm wavelength region, with a resolution of 2.8 nm at 700 nm, 8 nm at 1500 nm and 6 nm at 2100 nm. The spectral bandwidths of the RS-3500 are 1.3 nm at 700 nm, 3.5 nm at 1500 nm and 2.3 nm at 2100 nm, which are resampled to 1 nm to provide 2151 bands. A calibrated piece of sintered Polytetrafluoroethylene (PTFE, also known commercially as Spectralon or Fluorilon) was used as the reflectance standard and measured before each set of soil measurements. The samples were measured with a bifurcated probe with a halogen light source. Each sample measurement consisted of 10 scans, averaged into a single measurement. Spectra were processed using The Spectral Geologist (TSG™) software to extract the main features reported as part of the UltraFine+® output (Table 1).

Final data for the Jericho project area was reprocessed in TSG™ with version 3.2 of the VNIR-processing template and may differ from previously reported, unrefined outputs.

2.2.6 Fourier transform infrared spectroscopy (FTIR)

No FTIR data was available for the Jericho project.

2.3 Automated QA/QC

The UltraFine+® Next Gen Analytics workflow has developed automated QA/QC on standards and duplicates for all available analyses, whereby analysis batch quality and internal reproducibility as recorded by standard and duplicate measurements can be assessed via a “traffic light system” which indicates the level of accuracy (standards) and precision (standards and duplicates) of the analyses.

Neither duplicate nor standard analyses were available for the Jericho project. Therefore, QA/QC could not be carried out.

2.4 Machine Learning - Spatial data integration and clustering

The UltraFine+® Next Gen Analytics workflow applies unsupervised dimensional reduction and clustering methods to spatial feature data to derive proxy landscapes. These and a range of other spatial outputs are designed to aid a first-pass interpretation of soil analysis results in a broader landscape context.

2.4.1 Spatial data clustering

The UltraFine+® Next Gen Analytics workflow uses semi-automated, unsupervised machine learning (ML) methods to cluster publicly available spatial data to define proxy regolith types. The spatial data layers used in this workflow were selected for their inferred relationship to regolith landforms and can provide information on landscape position, depth of transported cover, and parent and regolith material while minimising the introduction of human subjectivity, which would be the case by including surface geology or regolith landscape type maps. Spatial data layers included in the workflow are a Digital Elevation Model (the Copernicus GLO-30 Digital Elevation

Model), Multi-resolution Valley Bottom Flatness (MrVBF), Radiometric K %, Th (ppm), U (ppm) and barest Earth Sentinel-2 satellite data (Table 2). Sentinel-2 satellites, launched via the European Union Copernicus Program's Earth observation mission, collect high-resolution multispectral imagery data of the Earth with a revisit period of 10 days (see Digital Earth Australia data product documentation). The Sentinel-2 data used in this workflow is cropped from the Sentinel 2A Barest Earth Analysis Ready Data based on the soil sample locations. Ten out of thirteen spectral bands are collected: B02, B03, B04, B05, B06, B07, B08, B8A, B11, and B12. A three-component band ratio image is generated from the Sentinel-2 imagery (approximating the equivalent Landsat-7 ETM+ arrangement of Gozzard 2005; see USGS comparison of band equivalence here), with respective RGB bands calculated using R= B11/B12, G=B08/B12 and B=B08/B03.

Table 2: Spatial data layers used for landscape clustering for the Jericho project areas.

LAYER	LANDSCAPE INFORMATION	RESOLUTION [M]	DATA SOURCE
DEM	Landscape Position	**30**	Copernicus GLO-30 Digital Elevation Model was accessed on 11/05/2022 from https://registry.opendata.aws/copernicus-dem.
MrVBF	Depth of transported cover	**31**	Gallant, J., Dowling, T., Austin, J., 2012. Multi-resolution Valley Bottom Flatness (MrVBF). v3. CSIRO. Data Collection. https://doi.org/10.4225/08/5701C885AB4FE
Radiometrics K pct	Parent material	**110**	Poudjom Djomani, Y., Minty, B.R.S., 2019a. Radiometric Grid of Australia (Radmap) v4 2019 filtered pct potassium grid. Geoscience Australia, Canberra. http://dx.doi.org/10.26186/5dd48d628f4f6
Radiometrics Th ppm	Parent material	**110**	Poudjom Djomani, Y., Minty, B.R.S., 2019b. Radiometric Grid of Australia (Radmap) v4 2019 filtered ppm thorium. Geoscience Australia, Canberra. http://dx.doi.org/10.26186/5dd48e3eb6367
Radiometrics U ppm	Parent material	**110**	Poudjom Djomani, Y., Minty, B.R.S. 2019c. Radiometric Grid of Australia (Radmap) v4 2019 filtered ppm uranium. Geoscience Australia, Canberra. http://dx.doi.org/10.26186/5dd48ee78c980
Sentinel-2	Surface material and dispersion	**20**	**Digital Earth Australia** https://explorer.sandbox.dea.ga.gov.au/products/s2_barest_earth

The total area modelled for the Jericho project site was 3 km^2. Prior to dimensionality reduction and clustering all data layers were re-gridded to the highest input layer resolution (20 m) and scaled according to zero median and unit inter-quartile range. The dimensionality reduction algorithm UMAP (Uniform Manifold Projection and Approximation; McInnes et al. 2018) was applied to project the data into a three-dimensional latent space (a representation of data compressed to three dimensions, in which similar data points are closer together in space; Figure 4) for more efficient clustering and provide a framework for visualisation. The UMAP algorithm was used as it captures non-linearities within the data and preserves local structures. The method does not explicitly include any location information, spatial relationships, or spatial features (e.g., textures) as only the per-pixel values of each input layer were considered.

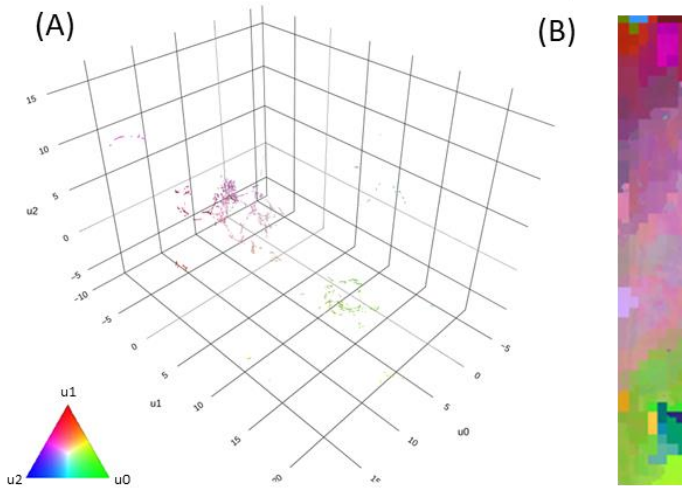

Figure 4: (A) Scatter diagram of pixel values for the Jericho project site embedded in a 3-dimensional latent space using the dimensionality reduction algorithm UMAP. Points are coloured using an RGB of the axes (u0, u1, u2) values. (B) Pixel values projected into 2-dimensional space for spatial context over the Jericho project area.

K-means and agglomerative (hierarchical) clustering algorithms (scikit-learn implementation in Python; Pedregosa, 2011) are used in the UltraFine+® Next Gen Analytics workflow to cluster locations with similar remotely sensed spatial data signatures after reduction with UMAP. Both clustering techniques force all sample points into a given number of clusters. Due to the intended application of the clustered proxy landscape types to geochemical sample interpretation and the added complication that these landscape models are intended to be used over a variety of area sizes (1 km^2 to 50,000 km^2) the number of clusters has been predetermined for the workflow. Four clusters are routinely used for *k*-means (for project areas <20 km^2) and eight clusters are routinely used for agglomerative clustering (for project areas >20 km^2). Herein, we term these 'kmeans4' and 'agg8'. Note that since October 2022, a third clustering algorithm (agglomerative clustering with 12 clusters) was added to the workflow. However, due to the very small area size of the project site, we have not included these results here, to reduce the size of the data package.

K-means is an iterative clustering algorithm that randomly selects a cluster centre from a dataset to compute distances of all data points from this selected centre, from which it calculates a new centre point. This is repeated until four centroids (geometric centres) with maximum distance from each other have been sampled. During each iteration, all data points are subsequently assigned to the closest cluster centre based on their Euclidean distance in the multi-dimensional space. The algorithm then calculates the average of all points in each cluster and moves the centre point to this location (MacQueen, 1967).

Agglomerative clustering is a hierarchical clustering algorithm that recursively merges pairs of clusters, which minimise a distance metric. We use the scikit-learn default, Ward linkage criterion, which minimises the variance within newly merged clusters. Training an agglomerative clustering model is computationally intensive and, once trained, a model is not able to assign new samples to established clusters. To assign cluster labels to pixels at a larger scale, a multi-step process was used:

a) fit an agglomerative clustering model using a random subset of 20,000 pixels,

b) use this same subset and their cluster labels (from step 1) to train a random forest classifier; and

c) use this classifier to predict cluster labels for all pixels across the area of interest.

The random forest classifier is a very good proxy for the agglomerative clustering model, with out-of-bag (OOB) performance typically above 99% accuracy. For areas smaller than 20,000 pixels, such as Jericho, the agglomerative clustering model is used directly, however, for larger areas such as the broader region considered in Section 3.1.3, the process described above was used. Once all data points are clustered, a colour is assigned to each cluster with similar projected spatial features (Figure 5; colours are assigned based on mean cluster MrVBF values). These clusters can be plotted by cluster colour according to their corresponding spatial reference (Figure 6G, H) to generate maps which are used to evaluate the proxy regolith type that each cluster corresponds to. These maps are outputted as GeoTIFF files (see Appendix A) as well as PNG files (see Section 3.1).

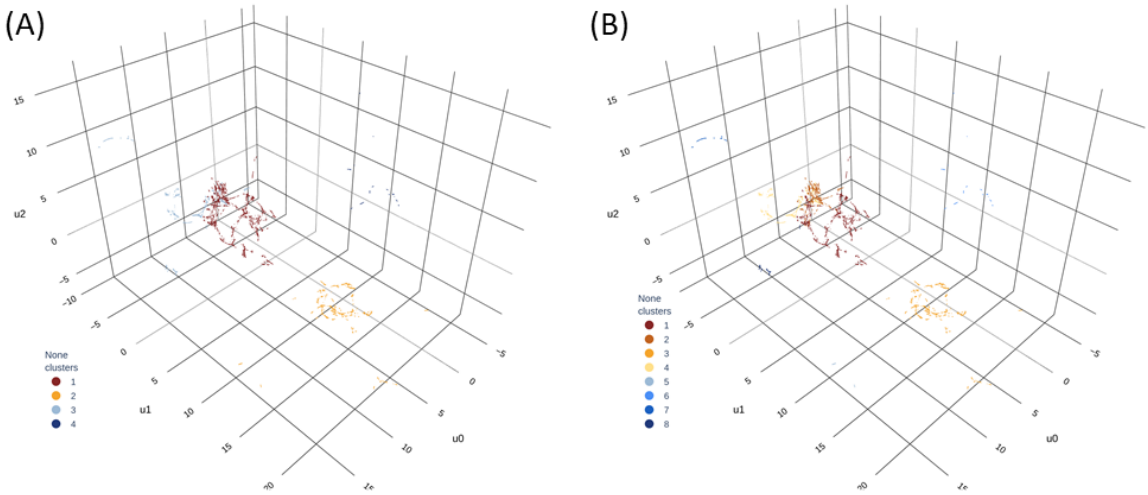

Figure 5: Clustered pixels of GSQ's Jericho project site in the 3-dimensional latent space grouped by cluster colour to visualise data separation. (A) Pixels clustered into four clusters using the *k*-means algorithm (kmeans4). (B) Data points clustered into eight clusters by an agglomerative clustering algorithm (agg8). Refer to Appendix A for an interactive plot of these scatter diagrams.

2.4.2 Geochemical outliers by landscape type

Prior to identifying outliers within the geochemical dataset, all values below the detection limit were replaced with half the detection limit value for each respective element. Elemental outliers were calculated on log-transformed data and are defined as values that are greater than 1.5 times the first and third interquartile range. Geochemical data were also grouped by their corresponding landscape cluster and outliers were calculated for each of these clusters. The workflow automatically produces boxplots for each element by landscape type (i.e., cluster), as well as in spatial context plotted over a landscape cluster map for each element (see section 3.3). In addition, shapefiles with outliers grouped by element and landscape type are produced. The data is also available as a CSV file (see Appendix A).

2.4.3 Principal Component Analysis

Principal Component Analysis (PCA) is performed on centred-log-ratio transformed and quantile-normalised geochemical data for each soil sample. All values below the detection limit were

replaced with half the detection limit value for the respective element. The workflow reduces each data point (soil sample) from *n* dimensions (number of analysed elements) into five principal components (PC0 to PC4) while preserving the maximum of information. The explained variance (importance) of the principal components decreases from PC0 to PC4. For each principal component, the loading (influence) of each element is plotted on a spider diagram to illustrate the general geochemical affinity (see Section 3.4.1). The spatial distribution of samples coloured by the weight of the principal component is also available (see Section 3.4.1). A threshold of 10 % is applied for missing data points (due to non-analysis) to determine if an element is included in the PCA analysis. If less than 10 % of data points of a given element are missing, the element is included in the PCA analysis, but no principal components are calculated for the affected sample.

2.4.4 Regolith ratios and indices

Multi-element indices and regolith ratios based on common examples used in Australian exploration settings were calculated from soil sample geochemical data (see Appendix 1). These include indices for the purposes of normalisation (e.g., Au/OrgC) as well as indicators and proxies of mineralisation (e.g., CHI6). All geochemical values below the detection limit were replaced with half the detection limit value for the respective element prior to transformation and calculation of indices. Multi-element compositional indices are derived from centred-log-ratio (CLR) transformed geochemical data for each soil sample (addressing proportional dependence related to closure; additive components in log-ratio space are roughly equivalent to multiplicative components in compositional space). Regolith ratios were calculated from measured elemental abundances (without further transformation), sizing data and/or spectral analyses of ultrafine soil samples.

2.4.5 Soil sizing

Particle size analysis was conducted on field samples (<2 mm; dried soil) with the results reported in percentage of sand, silt and clay. These values are plotted in a ternary plot commonly used in soil science to provide a general textural class (Soil Science Division Staff 2017). Plots were generated using pyrolite (Williams et al. 2020) and symbolised by colour according to broad soil textural classes (e.g., sandy loam, silty clay). These classes are presented on the soil textural triangle and in spatial context allowing users to see key changes in the landscape soil morphology (see Section 3.5.2).

2.4.6 Dispersion and source direction

Dispersion/source direction and topographic slope are extracted at each point from Australia-wide slope (Gallant and Austin 2012a) and aspect (Gallant and Austin 2012b) datasets, which were derived from a smoothed version of the SRTM DEM processed to reduce noise. Dispersion direction indicates the direction in which the land surface slope faces (i.e., the aspect) and is generated on a grid over a given project area. Source direction is the opposite of this (i.e., upslope direction) and is generated for each sample point. Outputs are available as shapefiles with associated layer files that display both source and dispersion direction as scaled arrows (see Appendix A). The size of the arrow is proportional to the slope degree.

3 The UltraFine+® Next Gen Analytics Outputs

The UltraFine+® Next Gen Analytics workflow uses machine learning to integrate spatial data and soil properties in several derived outputs. For each project area, these outputs include proxy regolith landscape clusters for a given project area, maps and boxplots of elemental outliers by landscape type, principal component analyses, soil texture diagrams, source and dispersion directions, regolith geochemical indices and catchment analysis. At the time of writing this report catchment analysis was still under development and will be applied to stream sediment sample surveys only. As a result, these parameters will not be reported for the Jericho samples. Most outputs are available in GeoTIFF, PNG, shapefile and CSV formats. Please refer to Appendix A for available outputs contained in the GSQ project data package.

3.1 Landscape clusters

As part of the UltraFine+® Next Gen Analytics workflow, spatial data clustering is used to derive proxy regolith types to provide landscape context for geochemical samples. These proxies are derived from spatial data only (i.e., MrVBF, DEM, radiometric data, and Sentinel-2 derived regolith ratios) and are not based on physical soil sampling. A variety of clustering methods with varying numbers of clusters (proxy landscape types) have been trialled in several locations across the Australian continent, with the aim to develop semi-automated landform mapping that is applicable over a wide range of settings and project sizes. The standard data package includes "kmeans4" (a four-cluster *k*-means clustering) for small areas (<20 km^2) "agg8" (an eight-cluster agglomerative hierarchical clustering) for larger areas (>20 km^2) and "agg12" (a twelve-cluster agglomerative hierarchical clustering) for larger areas with dense sampling. All outputs of the workflow are automatically generated for all three algorithms. However, agg12 has not been included in the Jericho Project Data Package (Appendix A) due to the very small area size and minimal sampling across the area. Optimising and ground-truthing the UltraFine+® Next Gen Analytics workflow for application on all scales and for a variety of landscapes across the Australian continent as well as a trial site in New Zealand (Figure 1) is part of ongoing research.

3.1.1 Comparison of unsupervised clustering methods

Since the UltraFine+® Next Gen Analytics workflow is designed primarily for interpretation of soil samples prior to significant ground disturbance in a greenfield exploration setting, anthropogenic infrastructure such as major roads, built-up areas, as well as mining- and agriculture-related infrastructure are usually masked to be excluded from the landscape models, as these can influence the spatial input layers (e.g., spectral band regolith ratios derived from Barest Earth Sentinel-2 data). However, given that the small Jericho project area is adjacent to an active mine site and a heavily trafficked road passes through the project area, masking was not applied. The potential influence of surface disturbance on the machine learning derived landscape cluster outputs should be considered when using workflow outputs for data interpretation.

For the Jericho project site, both the *k*-means and agglomerative clustering algorithms provide a more detailed landscape context than publicly available interpreted regolith and surface geology products, which show one (regolith geology) and three (surface geology) units, respectively (Figure 6E, F). Due to the small scale of the project area, the main features (maximum variation) of the input layers (Figure 6A-D) captured in the agglomerative clustering algorithm (with 8 clusters; Figure 6H) are too detailed given the limited number of soil samples.

A comparison of the machine learning derived landscape clusters with input layers (Figure 6 and Figure 5A-D) show that the main features are well represented with the four landscape clusters derived via the *k*-means algorithm. The UMAP 3D scatter plot shows distinct low density clusters (Figure 4A; similar data points are closely positioned together in a 3-dimensional space) separated in space from each other, which may warrant further discrimination (e.g., 8 clusters) not readily discernible by the human eye from input layers (Figure 6A-D). However, given the sparse soil sample density across the very small project area, this does not relate to proxy regolith type separation useful in the current exploration context.

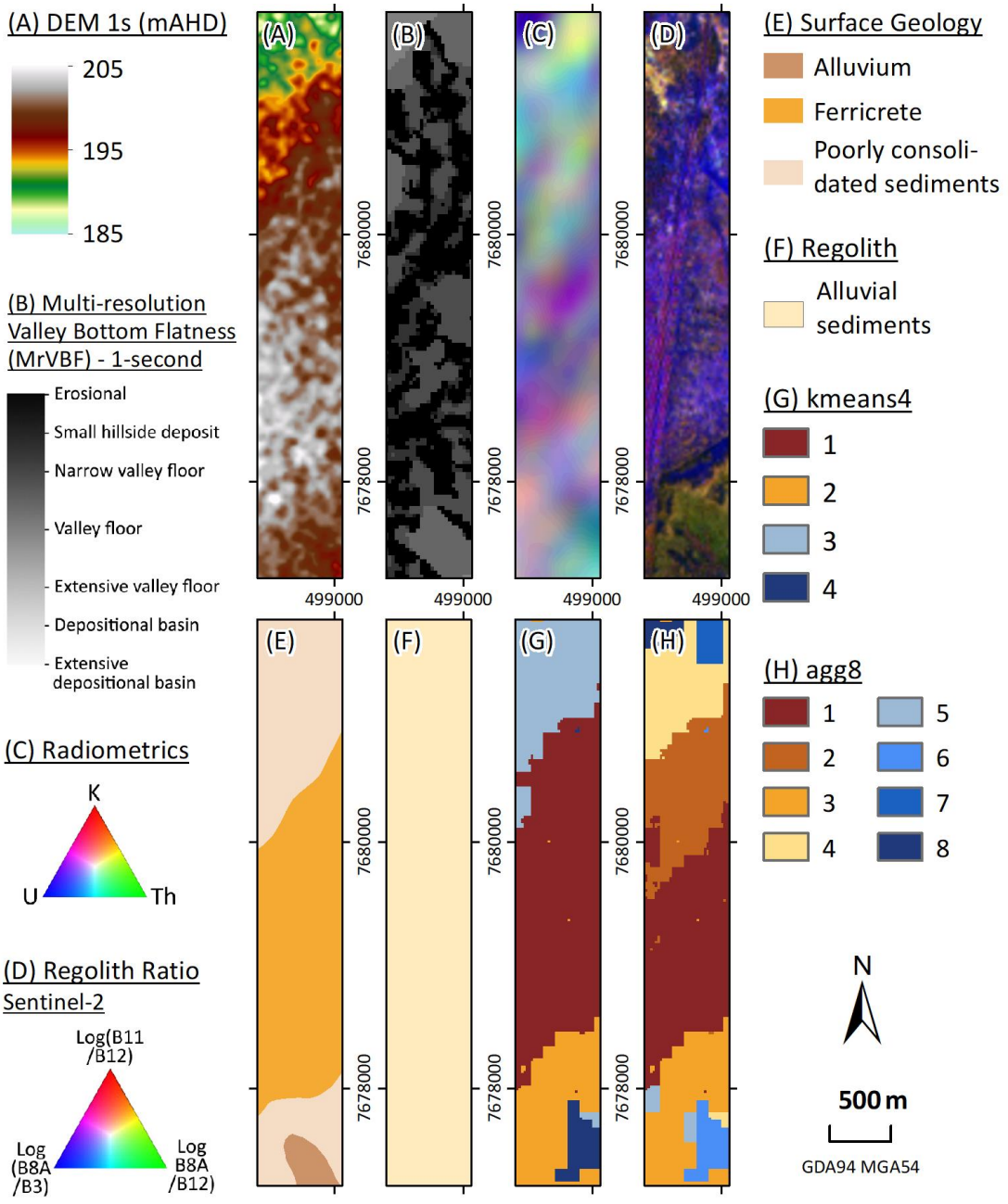

Figure 6 (previous page): Proxy regolith clustering input layers (A-D) and comparison of traditional geological maps (E, F) to machine learning derived outputs (G, H) over the Jericho project area. (A) 1-second DEM SRTM (Gallant et al. 2011). (B) Continuous MrVBF (Gallant et al. 2012). (C) RGB image of radiometric grid of Australia (Poudjom Djomani and Minty 2019a-c). (D) RGB image of sentinel-2 regolith ratios (derived after Gozzard 2005). (E) Surface Geology (Department of Resources 2018) (F) Regolith Geology (Geoscience Australia 2013). (G) Proxy regolith types derived via *k*-means with four clusters plotted in spatial context. (H) Proxy regolith types derived via agglomerative clustering with eight clusters plotted in spatial context.

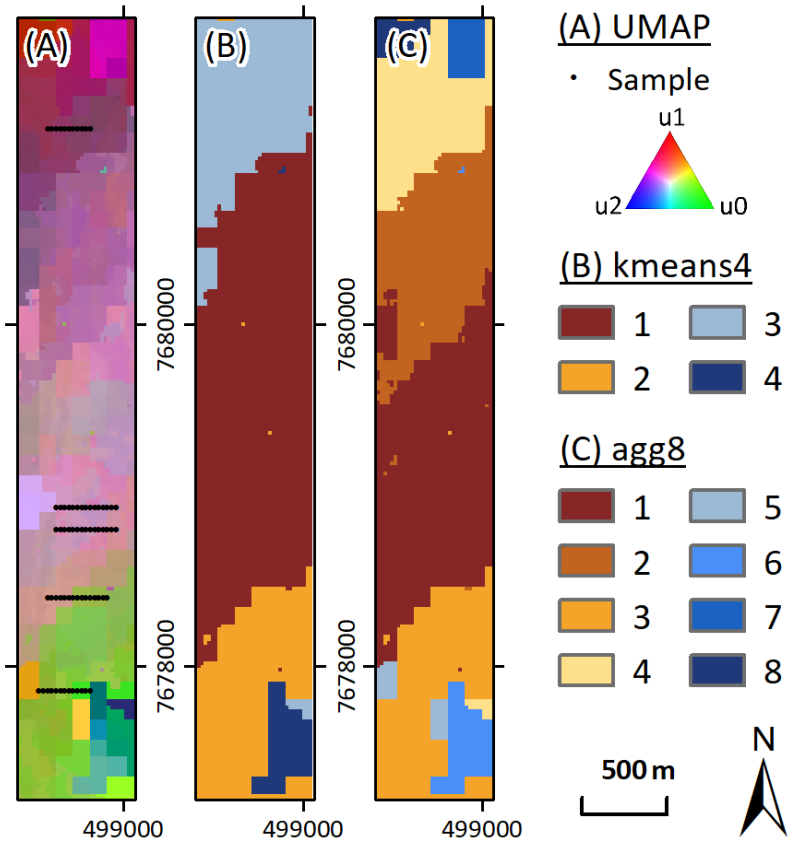

Figure 7: Comparison of dimensionality reduction and clustering algorithm outputs plotted in spatial context over the Jericho project area. (A) Spatial representation of cluster similarities in RGB colours derived via the dimensionality reduction algorithm UMAP; the more similar the colour, the more similar the spatial characteristics of the data points. Subsequent landscape cluster outputs are derived from this output and, in general, the closer they match the UMAP distribution, the more representative these clusters are. (B) Landscape clusters derived via *k*-means clustering with four clusters. (C) Landscape clusters derived via agglomerative clustering with eight clusters.

3.1.2 Landscape types in the Jericho project area

While the unsupervised landscape clustering approach does not assign a particular regolith type to a cluster (see three-dimensional projection in Figure 4A), the spatial representation of these clusters corresponds well with broad landscape patterns in the project area (Figure 6 and Figure 7). Therefore, proxy regolith types for the project areas can be interpreted from the landscape clusters by comparing each cluster to the input layers (Figure 6A-D and

Figure 9A-D). In addition, the clusters were also compared to publicly available surface geology (Figure 6E and

Figure 9F) and regolith geology (Figure 6F and

Figure 9G). It is important to note that these regolith proxies are generalised descriptors aligning with most of the landscape features within a cluster and no ground-truthing was undertaken for the project area. However, we highlight below several examples of the overall positive alignment of landscape clusters with the input layers and take note of some of the constraints.

Overall, both kmeans4 (Figure 8A) and agg8 (Figure 8B) outputs are useful regolith proxies for the Jericho project area and provide more landscape context than publicly available surface geology and regolith maps (Figure 6F, G). The four-cluster *k*-means clustering output is recommended for the project area given the small site area and the constraints around the number of samples per landscape clusters. The four landscape classes depicted in the kmeans4 output very closely match the surface geology (

Figure 9E) as well as the different soil types noted in the Australian Soil maps and described above (Isbell 2012) and a review of these proxy regolith types indicates that all are depositional landscape settings.

Ferricrete soil (landscape cluster 1)

The dark red-brown landscape cluster 1 very closely matches the slightly elevated (

Figure 9A) ferricrete cemented alluvium in the surface geology map (

Figure 9E, I). Commonly, this may be viewed as a residual landform, but in this region and others, ferricretes can be inverted landforms previously formed in channel environments and more representative of (ancient) depositional settings. Hence it is important to designate this as ferricrete but not as residuum. We term this proxy regolith type here as ferricrete soil (Figure 8A).

Sand plains (landscape clusters 2 and 3)

Sand plains are noted in the project area with landscape cluster 3 (grey-blue) in the north and landscape cluster 2 (orange) in the south of the project area (

Figure 9I). Both appear to be sand plains in satellite imagery (

Figure 9E, J) although it is difficult to determine without ground-truthing and both are mapped as unconsolidated material in the surface geology map (

Figure 9E). The project area is small with little obvious landscape features and landscape cluster 2 (orange) is likely similar to cluster 3 in topography. However, landscape cluster 3 (grey-blue) has a slightly more elevated landscape position (

Figure 9A) with a change in underlying parent and regolith material, as evident in radiometric data (

Figure 9C) and spectral band regolith ratios RGB imagery (

Figure 9D). A change in geology to the south and increase in carbonate materials in landscape cluster 3 (orange) was also indicated in UltraFine+® soil analyses (see Sections 3.4 and 3.5). Both clusters show greater weathering intensity within the project area than landscape clusters 1 (dark red-brown) and 4 (dark blue) (Wilford and Roberts 2019;

Figure 9G).

Alluvial floodplain

Landscape cluster 4 (dark blue) is influenced by the MrVBF and reflects the potentially deepest, more recent, cover within the project area. However, the regolith in the Jericho/Eloise area is commonly thick and is not well reflected in the MrVBF data on a small scale. As a result, the dark blue landscape cluster 4 aligns with a more recent alluvial channel.

Agg8

Additional landscape classes provide the possibility to include secondary features, such as parent material, as reflected in the radiometric data (

Figure 9C). The agg8 (Figure 8B) output provides four more differentiated landscapes, which support the outputs seen in the kmeans4 model output, with a subtle separation of the ferricrete unit linked to some variation in the parent material sediments. Other units reflect gradations into the alluvial channel or changes in the radiometric response to different possible sources of sediments. The maximum variation of any input layer usually influences which landscape cluster a given data point is assigned to. This means that, where a model is set to only four landscape clusters and depth of cover is the parameter with the maximum variation, this feature will be defining. At the Jericho site the Sentinel-2 derived regolith ratio (

Figure 9D) maps the main units, while radiometric data (

Figure 9C) indicates the ferricrete soils and a change in material as well as cover depth (MrVBF;

Figure 9B) at the south-eastern edge of the survey area.

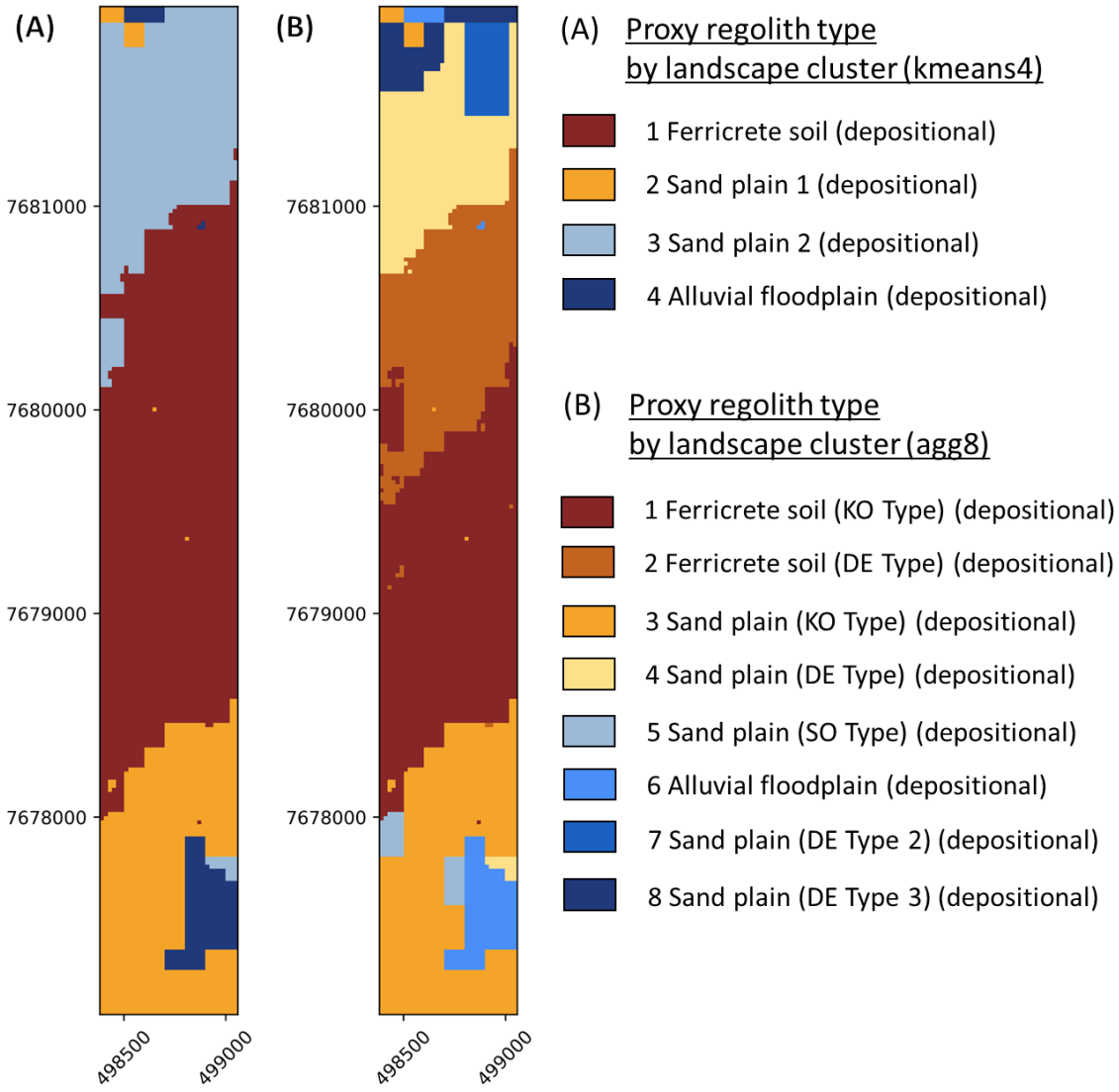

Figure 8: Correlation of proxy regolith types with landscape clusters for the Jericho project area generated by (A) a *k*-means clustering algorithm with four clusters (B) an agglomerative clustering algorithm with eight clusters. Please refer to the text for more detail on these proxy regolith types.

Figure 9 (next page): Spatial layers used for the interpretation of landscape clusters produced by machine learning over the Jericho project area. (A) DEM. (B) MrVBF as proxy for depth of cover. (C) Radiometric data as indication for differences in parent materials. (D) Spectral band regolith ratio as indication for differences in regolith materials. (E) Surface geology. (F) Regolith geology. (G) Weathering intensity. (H) Satellite imagery. (I) Landscape clusters derived via kmeans4. (J) Landscape clusters derived via agg8.

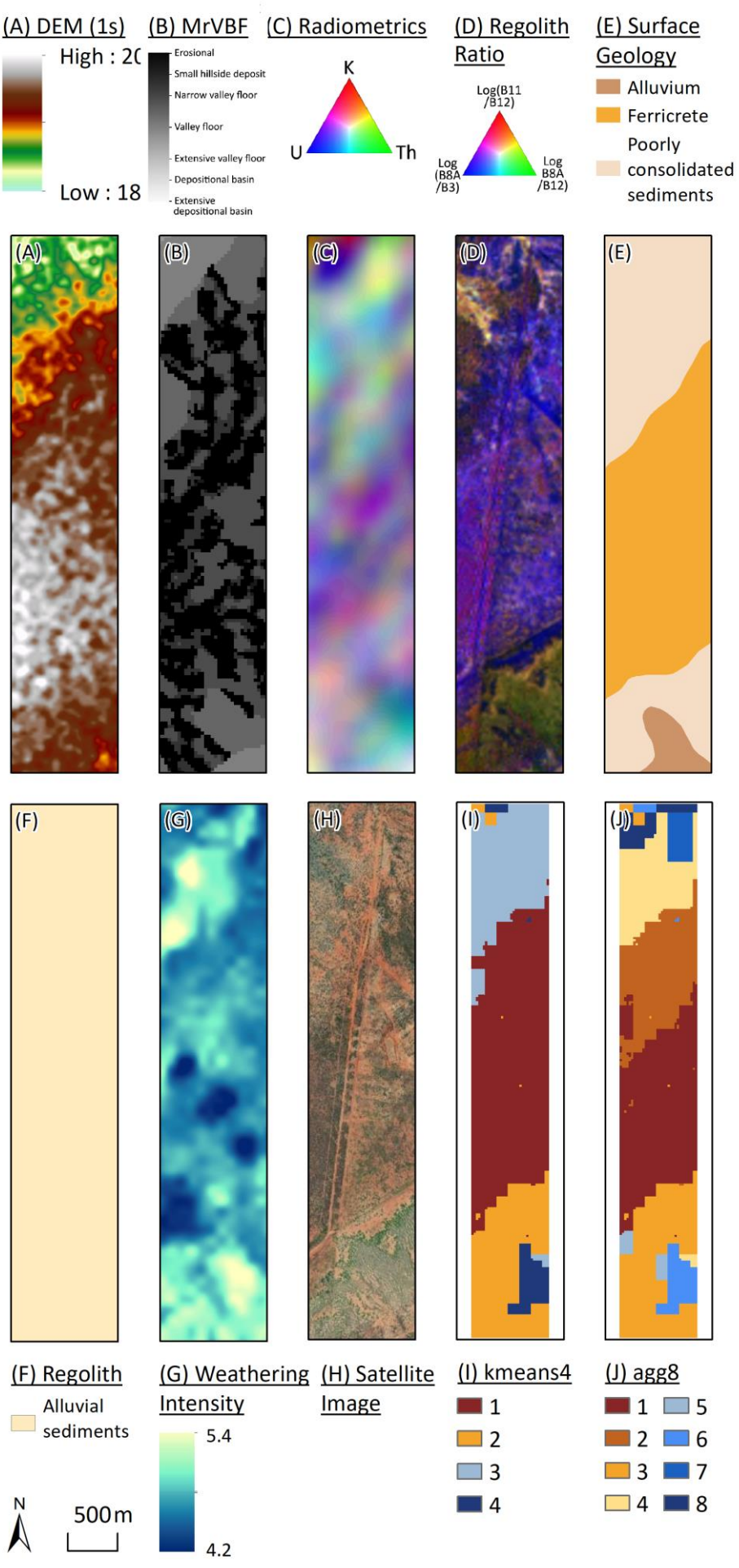
(A) DEM (1s)
High : 20
Low : 18
(B) MrVBF
Erosional
Small hillside deposit
Narrow valley floor
Valley floor
Extensive valley floor
Depositional basin
Extensive depositional basin
(C) Radiometrics
K
U
Th
(D) Regolith Ratio
Log(B11 /B12)
Log (B8A /B3)
Log B8A /B12)
(E) Surface Geology
Alluvium
Ferricrete
Poorly consolidated sediments
(A)
(B)
(C)
(D)
(E)
(F)
(G)
(H)
(I)
(J)
(F) Regolith
Alluvial sediments
(G) Weathering Intensity
5.4
4.2
(H) Satellite Image
(I) kmeans4
1
2
3
4
(J) agg8
1
2
3
4
5
6
7
8
N
500m

3.1.3 Broader landscape context for the Jericho region

The Next Gen Analytics workflow was designed to provide landscape context for greenfields exploration in shallow (<30 m) transported cover over areas with 100s to 1000s of samples. During this research project, the Jericho project site was one of the few sites to examine the limits of the workflow at the smaller end of project site scales in terms of area as well as sample numbers. These limitations are largely due to the resolution of the available input data as well as the likelihood of strong variety of landscape types. In areas such as this study site, where landscape type and cover depth are similar for each sample point, landscape context is less important.

To demonstrate the benefit of the machine learned landscape clustering approach for future exploration in Queensland, we generated a larger area (approximately 40 km x 40 km) landscape proxy map centred around the Jericho project area (Figure 10) with the standard agg12 (12 landscape clusters generated via an agglomerative algorithm following the methods above) regolith proxy output that is part of the UltraFine+® Next Gen Analytics data package for larger project sites.

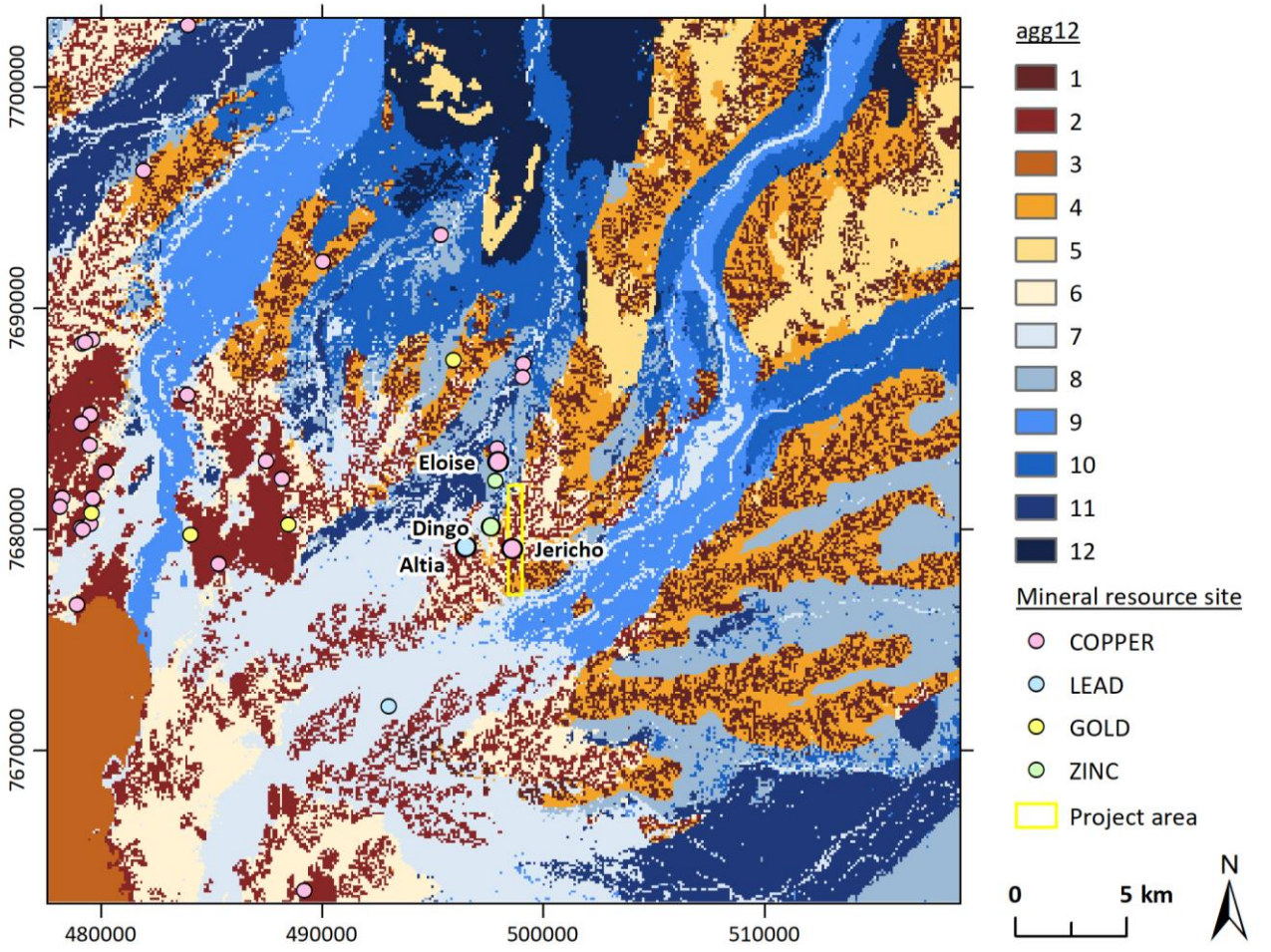

Figure 10: Proxy regolith clusters over the general Jericho region generated with an agglomerative clustering algorithm with twelve landscape clusters.

The available regolith geology map over this larger area differentiates three regolith types, saprolite, saprolith and, for the vast majority of the ~1,600 km^2, alluvial sediments (Figure 11C). Most mineral resources (small and very small mineral occurrences) are noted in saprolite, while Altia, Eloise and Jericho are all located within the undifferentiated alluvial sediments (Figure 10).

The surface geology provides some additional context, separating the alluvial sediments noted in the regolith geology into alluvium, sand plain and colluvium (Figure 11D). However, the machine learning derived landscape clusters successfully clusters the main differences in landscape position (elevation via DEM; Figure 11G), changes in parent material (compare light brown landscape cluster 3 with radiometric data in the southwestern part of the area; Figure 11A, E), relative depth of transported cover (compare darker brown and darker blue landscape clusters with darker (shallower) and lighter (deeper) shades in the MrVBF; Figure 11A, H) and regolith materials (e.g., compare alluvial channel deposits indicated in white in the spectral band regolith ratio with the light blue landscape cluster 7; Figure 11A, F). This provides a much more in-depth landscape context than publicly available maps and can guide survey planning as well as data interpretation. Proxy regolith types of this output are available as GeoTIFF and PNG files and can also be explored in the Digital Sample Observer (a HTML-based dashboard; refer to section 4) either as an overview of all three landscape models, or individually for each landscape output (4, 8 and 12 classes) with supplementary spatial data in Appendix B.

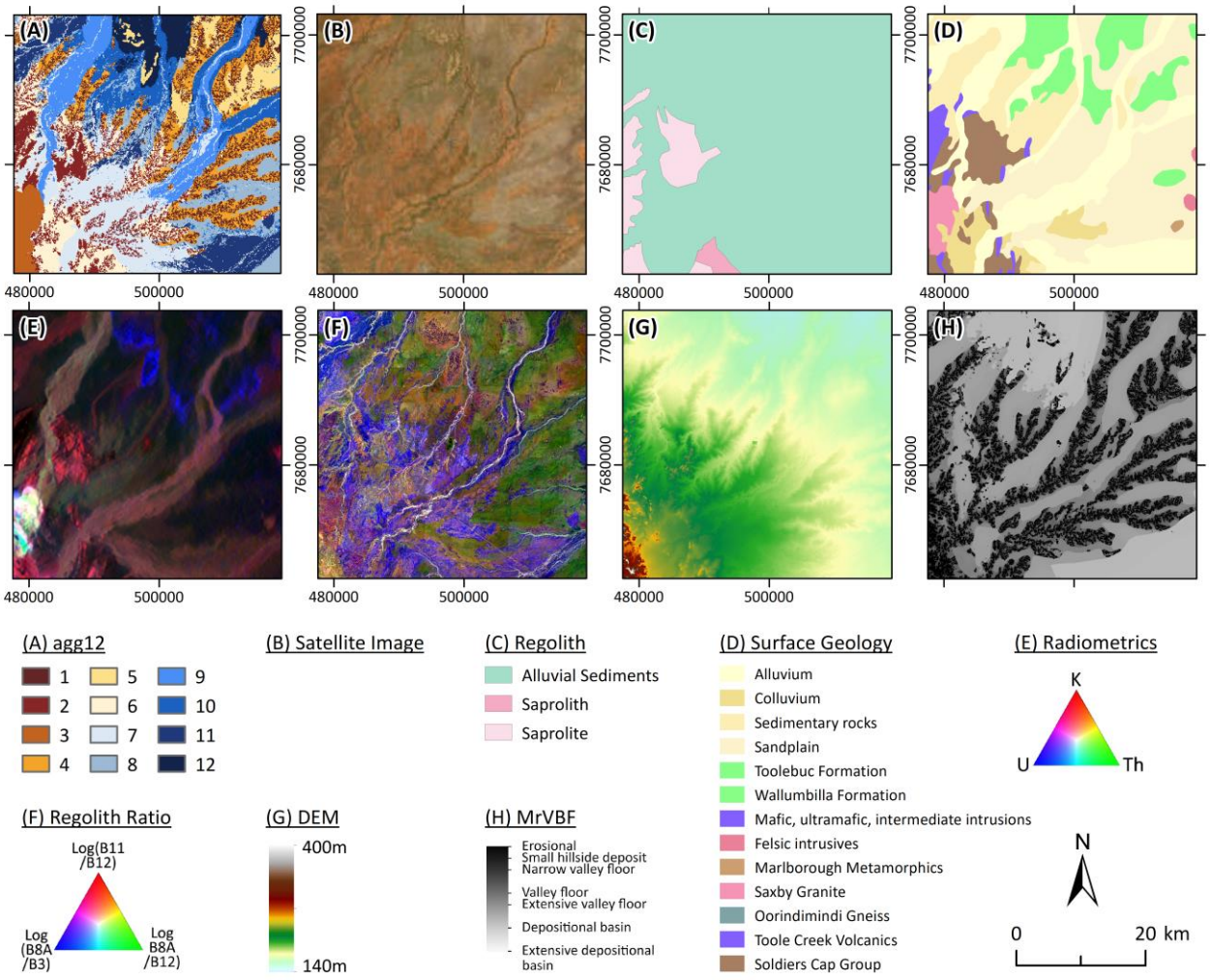

Figure 11: Proxy regolith landscape clusters, input layers and comparison to traditional geological maps over the general Jericho region. (A) Landscape clusters derived via agglomerative clustering with twelve clusters. (B) True-colour satellite image. (C) Regolith geology. (D) Surface geology. (F) Radiometrics (indication of parent materials). (G) projection of spectral band regolith ratio (indication of regolith material). (H) Digital Elevation model (indication of landscape position). (H) MrVBF (indication of depth of transported cover).

3.2 UltraFine+® geochemistry results

The UltraFine+® soil analysis method is based on separating and analysing the ultrafine fraction (<2 µm) of a given sample, as most metals as well as some useful indicator elements in transported cover tend to adsorb preferentially to clay particles and other "scavenging" phases with large surface areas. By removing the bulk of the coarse-grained "barren" portion of the sample, the signal to background ratio is increased and nugget effects are removed. In addition, the analysis requires smaller sample volumes due to the enhanced sensitivity with up to 100 – 250 % increased concentrations of Au, Cu and Zn observed (Noble et al. 2018). The method is, therefore, well suited to leverage existing dispersion mechanisms during weathering in shallow transported cover. In general, exploration settings with mineralisation at depth of >30 m below transported cover, and/or mineralisation without a mechanism in place to transport a geochemical signature, will not be conducive to surface geochemical sampling. While surface geochemical techniques (including the UltraFine+® approach) are, therefore, not the preferred exploration approach over the Jericho deposit, this data was an essential part of the initial soil samples used to improve the UltraFine+® geochemical assays and develop the spectral analysis outputs. Since the commencement of the UltraFine+® Next Gen Analytics research project, the UltraFine+® soil analysis method has undergone continuous improvements based on samples submitted by project sponsors, such as state geological surveys, including the Geological Survey of Queensland. For geochemical data acquisition, the main objective was to improve detection limits. Since the data acquisition for the Jericho project site (August 2019), detection limits for 30 elements, including Cu and Ag, were improved. In addition, three elements, Pd, I and Br, were added to the multi-element suite (Table 3).

Table 3: Detection limits, minimum, maximum, mean and median values for available elements for the Jericho project. Values below the detection limit were replaced by half the detection limit prior to calculations, and values rounded to significant numbers according to the detection limit. Refer to Appendix A for the full data set. Detection limits in blue font are current as of November 2022. Differences in detection limits due to improvements in the methodology highlighted in bold. *Analyses added after acquisition of the Jericho project data.

Element	Unit	DL Aug-19	DL Nov-22	Min.	Max.	Mean	Median
Ag	ppm	0.01	**0.003**	0.03	0.26	0.06	0.05
Al	ppm	10	10	85100	126000	104859	105000
As	ppm	0.5	0.5	5.1	12.3	7.9	7.6
Au	ppb	0.5	0.5	0.8	16.5	3.7	3.3
Ba	ppm	0.2	0.2	102.0	1000.0	214.8	128.0
Be	ppm	0.2	**0.01**	1.9	4.1	2.8	2.8
Bi	ppm	0.1	**0.002**	0.2	0.4	0.3	0.3
Br*	ppm	N/A	**1**				
Ca	ppm	10	10	1210	15400	3890	2620
Cd	ppm	0.05	**0.004**	0.03	0.13	0.06	0.06
Ce	ppm	0.05	0.05	48.20	123.00	78.11	75.70
Co	ppm	0.2	**0.01**	9.0	35.0	17.9	16.8
Cr	ppm	2	2	48	70	59	58
Cs	ppm	0.1	**0.03**	3.9	7.1	5.5	5.4
Cu	ppm	0.2	**0.1**	29.0	55.3	39.4	38.7
Fe	ppm	100	**50**	55700	83000	71632	73000
Ga	ppm	0.05	0.05	19.50	40.90	28.12	27.70
Ge	ppm	0.05	0.05	0.43	2.07	1.04	0.83
Hf	ppm	0.02	0.002	0.05	1.03	0.51	0.52
Hg	ppm	0.05	**0.001**	0.03	0.07	0.03	0.03

Element	Unit	DL Aug-19	DL Nov-22	Min.	Max.	Mean	Median
I*	ppm	N/A	1				
In	ppm	0.01	0.001	0.05	0.10	0.08	0.08
K	ppm	10	10	4640	8810	6578	6440
La	ppm	0.05	0.05	21.00	64.50	42.67	43.50
Li	ppm	0.5	0.05	27.1	46.8	38.5	39.2
Mg	ppm	10	10	2560	13500	4687	3420
Mn	ppm	2	0.5	167	601	338	327
Mo	ppm	0.1	0.03	0.5	3.5	1.9	1.9
Nb	ppm	0.5	0.01	0.3	1.3	0.8	0.7
Ni	ppm	2	0.2	25	51	39	40
Pb	ppm	0.2	0.05	11.7	22.8	15.9	15.8
Pd*	ppb	N/A	1				
Pt	ppb	1	1	1	4	2	2
Rb	ppm	0.1	0.1	41.8	89.5	65.2	64.0
Re	ppm	0.01	0.0001	0.01	0.01	0.01	0.01
S	ppm	50	5	105	354	155	143
Sb	ppm	0.1	0.001	0.2	0.4	0.3	0.3
Sc	ppm	1	0.2	14	23	18	18
Se	ppm	0.05	0.05	0.30	1.44	0.65	0.63
Sn	ppm	0.2	0.02	1.9	3.3	2.6	2.6
Sr	ppm	0.1	0.1	72.1	150.0	91.1	85.1
Ta	ppm	0.01	0.001	0.01	0.02	0.01	0.01
Te	ppm	0.2	0.001	0.1	0.1	0.1	0.1
Th	ppm	0.02	0.02	8.10	21.90	14.29	14.40
Ti	ppm	10	2	899	1430	1098	1080
Tl	ppm	0.1	0.003	0.5	0.9	0.6	0.6
U	ppm	0.02	0.003	0.77	2.28	1.41	1.40
V	ppm	2	1	106	195	167	171
W	ppm	0.1	0.001	0.1	0.2	0.1	0.1
Y	ppm	0.05	0.005	14.60	45.30	25.78	25.00
Zn	ppm	0.2	0.2	39.9	60.2	47.7	47.2
Zr	ppm	1	0.1	2	42	27	28

Median concentrations for the main metals of interest in soil samples submitted for the Jericho project area were 50 ppb Ag, 3.3 ppb Au, and 38.7 ppm Cu (Table 3). No analyses for these elements returned values below the detection limit (DL). Silver concentrations ranged from 30 ppb to 260 ppb (DL = 10 ppb at time of data acquisition) with most of the highest values observed towards the west of the J1 lode in sample transects 1, 2, 3 and 5 (Figure 12A). Copper concentrations ranged from 29.0 ppm to 55.3 ppm with a diffuse distribution along sample transects but notably lower values along sample transect 5 (Figure 12B). Gold concentrations ranged from 0.8 ppb to 16.5 ppb (DL = 0.5 ppb) with highest values observed over and to the west of lode J1 along sample transects 1 and 2 (Figure 12C). While some elevated concentrations appear to coincide with the steeply west dipping lodes and there is possible potential for dispersion of metals upwards along shear systems, there is a lack of data to identify lateral background soil concentrations and/or information on dispersion mechanisms from depth to surface. Hence, these subtle elevated concentrations may be entirely coincidental. No background soil analysis data for the Jericho or Eloise deposits was available at the time of writing this report.

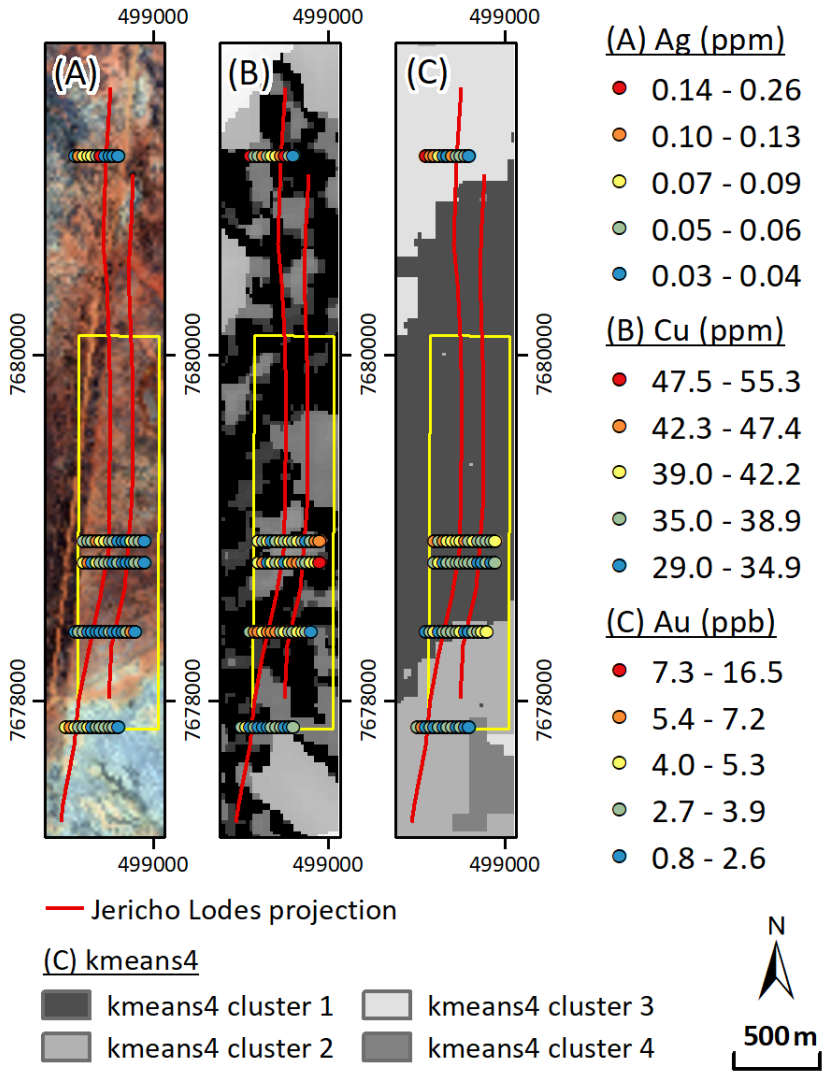

Figure 12: Spatial distribution of Ag (A), Cu (B), and Au (C) concentrations over the Jericho project area, with Jericho Lodes 1 and 2, as well as resource model area (yellow box) indicated.

3.3 Outliers by landscape type

Outliers in soil geochemical datasets are typically calculated based on all collected samples, regardless of their landscape context. However, this approach ignores the underlying processes that may affect metal dispersion. For example, high metal concentrations may be readily identifiable as outliers in a geochemical dataset where samples were collected over mineralisation beneath exposed outcrop or shallow residual materials, while the same mineralisation would have a much weaker elemental signal in samples collected over moderately thick depositional landscape settings. With the ability to approximate landscape types from spatial data via machine learning, the UltraFine+® Next Gen Analytics workflow can identify outliers within each individual landscape cluster (regolith proxy). This provides a basic, first-pass interpretation of geochemical samples by proxy regolith type and the identification of otherwise “overlooked” potential anomalies. The aim is to minimise overlooking mineral deposits in transported cover, which is common when targeting only the highest concentrations with little regard for changes in soil properties and landscape type. To this end, the workflow generates plots of log transformed results of all analysed elements by percentiles and separates these by regolith type.

While the Jericho project site was a valuable site for testing the first-generation UltraFine+® Next Gen Analytics workflow outputs in areas with known mineralisation and has aided in the refinement of the final project outputs, the Jericho project area does not contain a representative number of samples per landscape type for useful interpretation by proxy regolith type. In general, we consider the ideal minimum number of samples for statistically relevant analyses to be 50 and recommend disregarding the outliers generated by landscape clusters with less than 15 samples as these are not meaningful. As a precaution, outliers in clusters with less than 10 samples will not display on maps or in shapefiles generated with the UltraFine+® Next Gen Analytics workflow.

In addition, the Next Gen workflow was designed for greenfields exploration surveys, and the samples submitted over the Jericho project site run across the known Jericho lodes J1 and J2, without extending far enough to the west and east of the lodes to define the area's background geochemistry and, therefore, to identify outliers within the dataset.

Hence, the example in Figure 13 demonstrates the Next Gen Outliers by Landscape Type approach on the example of the Geological Survey of New South Wales's survey site in the Cobar region (Henne et al. 2022). In this example, traditional outliers calculated from all data as a single sample population are presented in the white box (Figure 13). In addition, the sample population is also grouped by landscape cluster and outliers calculated for each of these populations (coloured boxes). This highlights potential anomalies within different landscape settings (triangles below the dashed line). The dark brown and orange populations are from residual and/or erosional landscape settings and are therefore, as expected, well represented by outliers in the overall sample population (white box in Figure 13A). However, outliers in depositional settings (grey-blue and dark blue boxes in Figure 13A) would have been considered unremarkable if evaluated as part of the whole data set, demonstrating the benefit of evaluating the geochemistry in a landscape/regolith context.

While the UltraFine+® Next Gen Analytics workflow was designed to identify outliers in transported cover, the workflow accommodates for identifying anomalies in other settings by also generating data, maps and shapefiles for the whole sample population and, therefore, original, elevated elemental signals will not be lost. This should be considered when interpreting data where prospects are in areas of outcrop, subcrop or shallow residual soils.

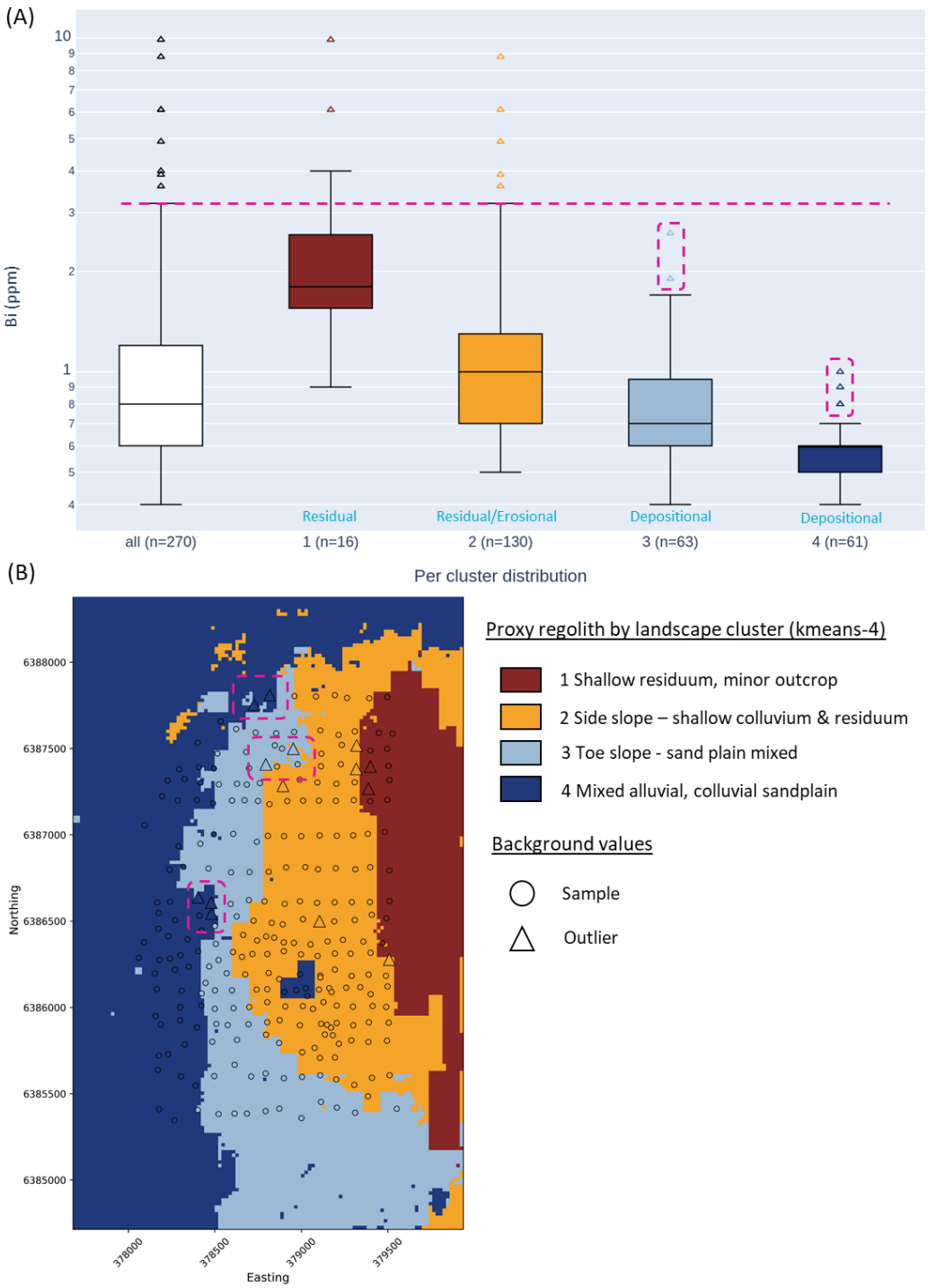

Figure 13: Example of machine learning derived outputs for outliers by landscape type over the Wagga Tank project area in NSW (Henne et al. 2022). (A) Boxplots for all Bi data (white box) and by landscape type (coloured boxes). Dashed line indicates the upper 25% boundary for the whole sample population. Easily observed soil anomalies are samples above the dashed horizontal line. Those shown below the dashed line would not be easily observed without the landscape context. (B) Spatial distribution of Bi outliers (triangles) by proxy regolith type. Outliers in dashed boxes correlate to outliers below the dashed horizontal line in (A) in depositional landscape settings. Note that the outputs have undergone minor cosmetic improvements (such as shading of boxplot background) for user-friendliness of the outputs since this example was generated and will therefore slightly differ for boxplots for the Jericho project site.

3.3.1 Outliers by landscape type - Jericho project area

The Jericho project area is located immediately south of the Eloise copper-gold mine and covers the Jericho Cu-Au deposit (Figure 2). The project area is also within 2 km of the Zn-Cu (Au-Ag) prospects Eloise South-West and Dingo, and the Pb (Ag-Zn-Cu-Au) prospect Altia.

As outlined above, the small area size with exclusively depositional landscape settings, as well as the number of samples per landscape cluster, limit the interpretation within landscape context over the Jericho project site. For the Jericho outputs generated via agg8, samples were only present in clusters 1, 3, 4, 5 and 6. However, populations in landscape clusters 4 (n=11), 5 (n=1) and 6 (n=1) are too small to be considered for meaningful interpretation and outliers are not displayed on maps. Landscape cluster 3 (n=19) should also be regarded with caution. Similarly, in the kmeans4 outputs, the sample populations for landscape clusters 2 (n=20), 3 (n=11) and 4 (n=1) are also too small to be considered for meaningful interpretation and outliers are not displayed on maps for clusters 3 and 4. Generally, within both the agg8 and kmeans4 outputs only landscape cluster 1 outputs are reasonable to be considered. Hence, samples should be assessed as a whole population instead. The below examples are, therefore, purely to demonstrate the outputs.

In each example for Au (Figure 14A), Ag (Figure 15A) and Cu (Figure 16A) the spatial distribution of outliers within the whole sample population are displayed as white triangles. Outliers for Au, Ag and Cu are mainly observed in soils from the northernmost sample transect with one additional outlier observed for Cu on sample transect 3. No outliers for either of these elements were identified by considering populations separately by four or eight landscape types (Figures 12 to 14B-E). Individual outliers not apparent from the whole-population analyses were identified by landscape types for exploration relevant elements such as Cd, Co, Cr, Mo, Pb, Sb and W (see boxplots in Appendix A). However, these do not provide relevant patterns with the limited context available.

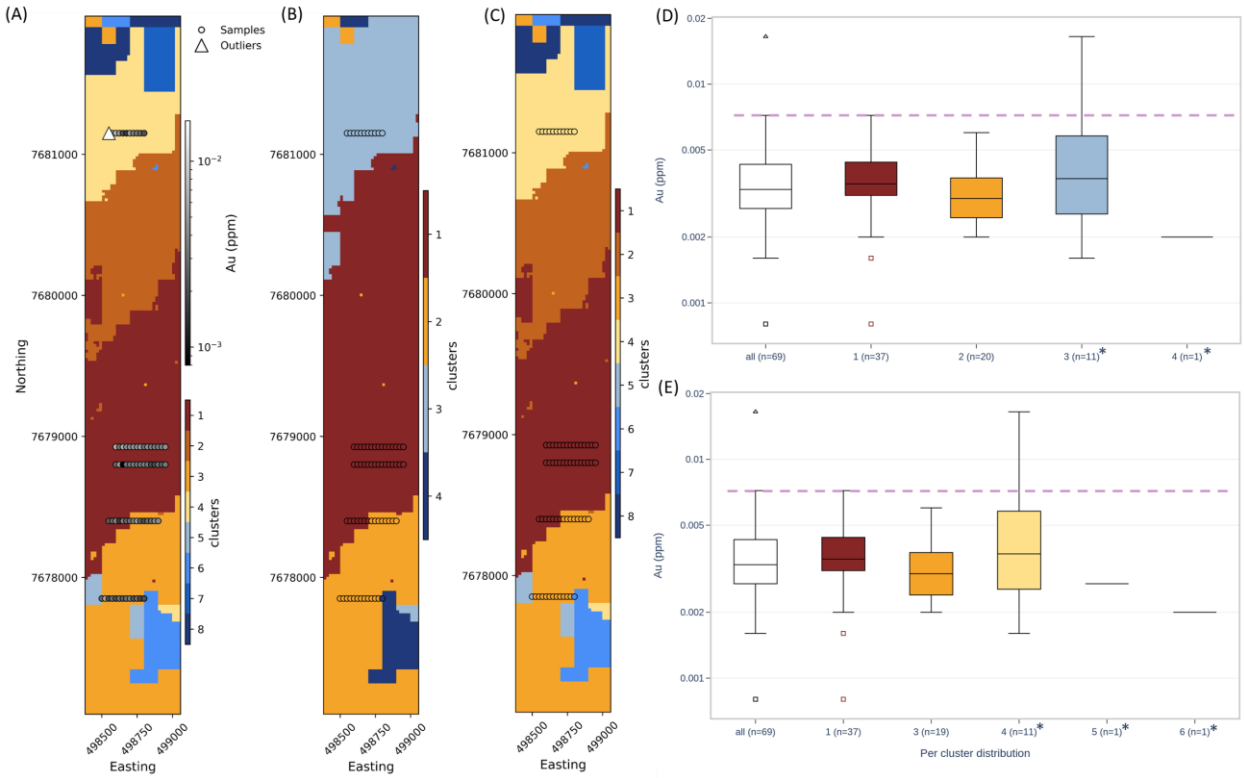

Figure 14 (previous page): Comparison of Au outliers in the whole sample population to Au outliers by landscape cluster over the Jericho project area. Outliers are plotted as triangles; no outliers by landscape type were identified. (A) Spatial distribution of Au outliers for all data. (B) Spatial distribution of Au outliers by landscape population with four clusters; no outliers were observed. (C) Spatial distribution of Au outliers by landscape population with eight clusters; no outliers were observed. (D) Boxplots for all data (white box) and by landscape type (coloured boxes) when calculated based on four landscape clusters. (E) Boxplots for all data (white box) and by landscape type (coloured boxes) when calculated based on eight landscape clusters. Easily observed soil anomalies are samples above the dashed horizontal line (white triangles in (D and E)). *Note that outliers in clusters with <10 samples will not display on maps as these are statistically not meaningful and outliers in clusters with <15 samples should also not be used for interpretation.

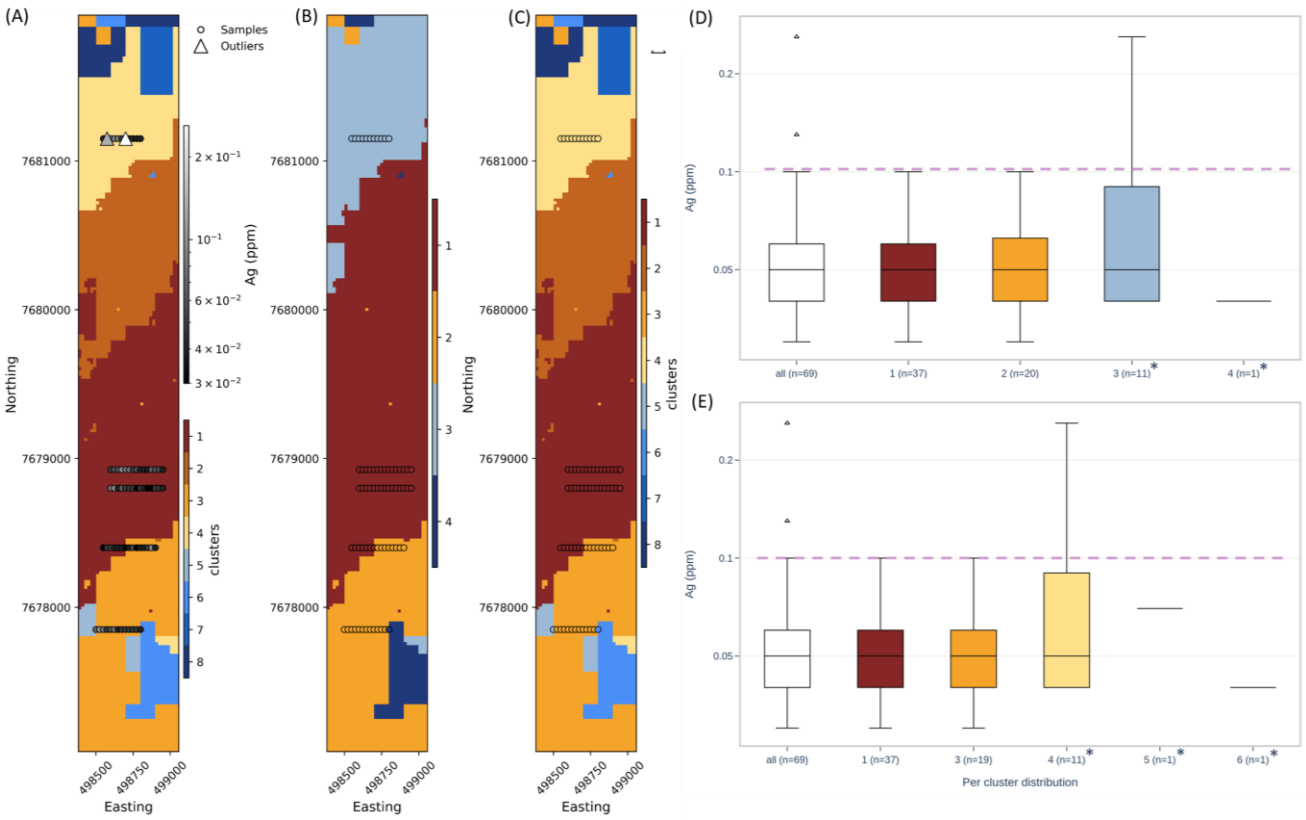

Figure 15: Comparison of Ag outliers in the whole sample population to Ag outliers by landscape cluster over the Jericho project area. Outliers are plotted as triangles; no outliers by landscape type were identified. (A) Spatial distribution of Ag outliers for all data. (B) Spatial distribution of Ag outliers by landscape population with four clusters; no outliers were observed. (C) Spatial distribution of Ag outliers by landscape population with eight clusters; no outliers were observed. (D) Boxplots for all data (white box) and by landscape type (coloured boxes) when calculated based on four landscape clusters. (E) Boxplots for all data (white box) and by landscape type (coloured boxes) when calculated based on eight landscape clusters. Easily observed soil anomalies are samples above the dashed horizontal line (white triangles in (D and E)). *Note that outliers in clusters with <10 samples will not display on maps as these are statistically not meaningful and outliers in clusters with <15 samples should also not be used for interpretation.

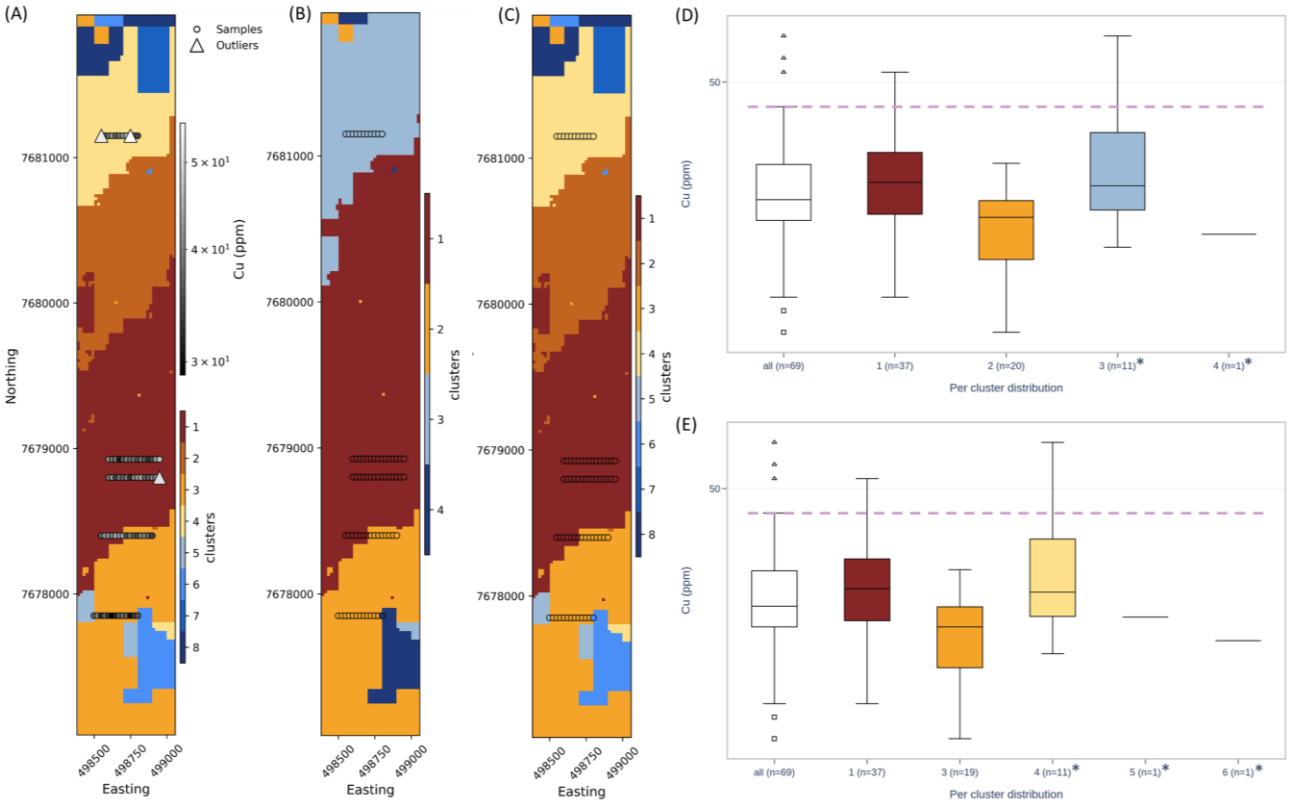

Figure 16: Comparison of Cu outliers in the whole sample population to Cu outliers by landscape cluster over the Jericho project area. Outliers are plotted as triangles; no outliers by landscape type were identified. (A) Spatial distribution of Cu outliers for all data. (B) Spatial distribution of Cu outliers by landscape population with four clusters; no outliers were observed. (C) Spatial distribution of Cu outliers by landscape population with eight clusters; no outliers were observed. (D) Boxplots for all data (white box) and by landscape type (coloured boxes) when calculated based on four landscape clusters. (E) Boxplots for all data (white box) and by landscape type (coloured boxes) when calculated based on eight landscape clusters. Easily observed soil anomalies are samples above the dashed horizontal line (white triangles in (D and E)). *Note that outliers in clusters with <10 samples will not display on maps as these are statistically not meaningful and outliers in clusters with <15 samples should also not be used for interpretation.

3.4 Exploration indices

The UltraFine+® Next Gen Analytics workflow derives exploration indices to automate the identification of patterns in geochemical datasets. Exploration indices via principal component analysis (PCA) are derived from all available elements without consideration of potential pathfinder suites or similar human interpretation. In addition, the workflow also derives regolith ratios and indices on a subset of elements based on decades of regolith and exploration literature of ratios and indices that are likely representative of specific mineralisation types. These outputs are designed for a rapid, first pass interpretation of geochemical results.

As is the case with the interpretation for the general geochemistry results and those for outliers by landscape type, exploration indices were designed for larger datasets in greenfield exploration settings and do not particularly suit the Jericho project data set. The below examples are, therefore, purely to demonstrate the outputs of the Next Gen workflow.

3.4.1 Principal Component Analysis

Principal component analysis is performed on quantile-normalised centre-log transformed data of all elements analysed for each soil sample. The automated output generates five principal components (PC0 to PC4). These principal components preserve the maximum variance between the samples while effectively reducing the number of dimensions. The loadings of each element for each of these five principal components are output in a spider diagram (Figure 17A). The further away an element plots from the zero line for a given principal component (coloured diamonds connected by coloured lines), the greater the loading for the specific principal component. The PCA allows for a rapid, first-pass identification of element association and potential exploration indices within the dataset. The spatial distribution of PCA-transformed sample data coloured by weight of the principal component is another output (Figure 17B). Principal component analysis for each sample is also available as shapefiles and CSV files, including eigenvalues, within the Jericho project data package (Appendix A).

While the importance (explained variance) of each of the principal components decreases from PC0 to PC4, principal components are often influenced by their landscape setting. Lower principal components will therefore typically pick out large-scale lithological variation as the major component(s). Principal components with exploration potential usually explain less variance in the data than the major elements related to bulk mineralogy. Hence, in many areas, PC2 and PC3 (3rd and 4th components) may represent the more relevant components in the context of mineral exploration. In some cases, signatures relating to mineralisation will constitute relatively low proportions of variance and thus not be represented by principal components. Further, signatures of mineralisation are typically localised spatially, and with most sampling patterns, contained to just a few samples – so by default these signals have lower chances of explaining large components of variance (PC0 or PC1) where most of the samples are 'background' but this background varies.

In the Jericho project area, the first principal component (PC0) explains 42.4 % of the variability within the dataset and is positively loaded with Ca, Mg, Ba and Sr (Figure 17A), reflecting the general change in soils at the southern edge of the project area, and indicates carbonaceous regolith materials with higher pH (compare Figure 17B to Figure 19A, C). Other principal components are positively loaded with a variety of pathfinder elements. However, given the context of deep cover and a lack of background geochemistry, the data does not support conclusive patterns for surface exploration purposes.

Figure 17 (next page): Principal Component Analysis outputs from the UltraFine+® Next Gen Analytics workflow over the Jericho project area. (A) Elemental loadings for each of the first five principal components. The further away an element plots from the 0 line, the greater the loading for (influence on) the specific principal component. (B) Output of the spatial distribution of principal components weighted by both colour and symbol size (absolute magnitude). The top five elemental loadings (greatest influence) for each principal component are indicated as headings. The colour red indicates a positive component weight (association); the colour blue indicates a negative component weight (association). The larger the symbols the stronger the association. From left to right, boxes display spatial distribution of principal component 0, 1, 2, 3 and 4 weightings.

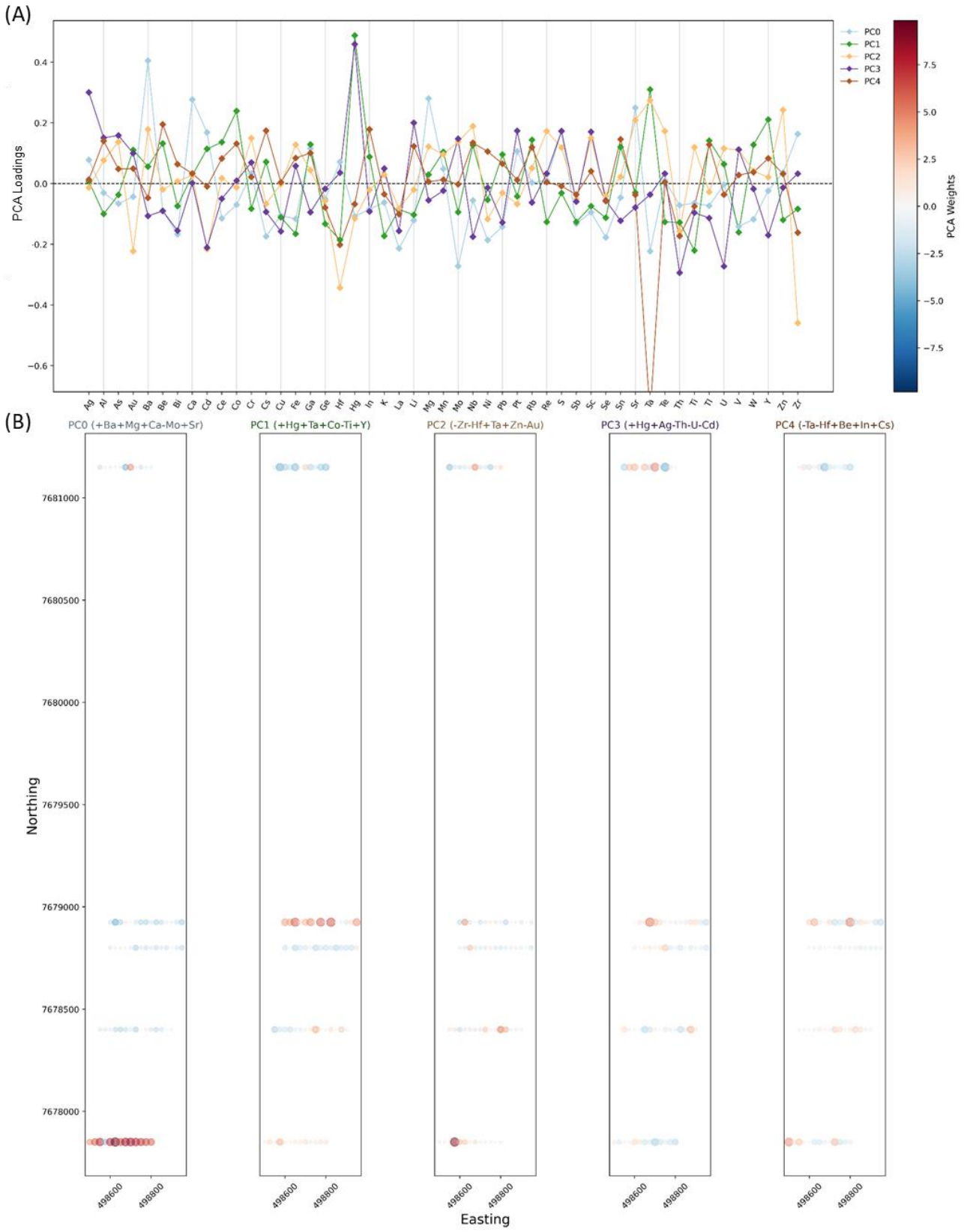

3.4.2 Regolith ratios and indices

The UltraFine+® method provides a high-quality, multi-element geochemical dataset as a standard output. With this wealth of information, geochemical data can be interrogated beyond the commodity of interest approach. The standard 52 elements as well as some of the additional soil

properties (e.g., total organic carbon and iron-oxide abundance) can be used to assess pathfinder elements associated with the main commodity of interest. This usually requires some general knowledge of mineral associations, dispersion mechanisms and weathering processes within the exploration area. While pathfinder suites can vary dramatically for different deposits, even of the same mineralisation style and within the same mineral province, general mineralisation style-specific regolith ratios and indices have been documented in exploration geochemical literature over decades. The Next Gen Analytics workflow leverages this knowledge by utilising the geochemical and spectral UltraFine+® analyses to generate a set of ratios and indices for each project site. These indices have been adjusted for available elemental compositions reported by the UltraFine+® method and indices (unlike ratios) are generated on centre-log ratio data. The indices and ratios are not intended to be an exhaustive list. Rather, the Next Gen Analytics workflow aims to provide common regolith ratios and simplified indices as an integrated output of the machine learning workflow with the aim to produce a first-pass assessment, at a glance, that can be interrogated spatially. The usefulness of a given pathfinder suite depends on ore forming processes, mineral assemblages and subsequent weathering processes. Ore zonation at depth can further complicate the applicability of fixed pathfinder suites and the geologist using this data is encouraged to make use of the extensive multi-element data and their local knowledge for a thorough interpretation of the data.

Due to the depth of cover and lack of background geochemistry, we present here the outputs for one regolith ratio and one exploration index for demonstration purposes only. The Next Gen Analytics workflow calculates 12 ratios (Table 4) and 22 indices (Table 5) ranging from gold pathfinder suites, porphyry and CHI6 indices, to pegmatite and greenstone indices for each soil sample. These are output as a CSV file, shapefile, as well as maps as JPG files, and can also be viewed in the Digital Sample Observer (see Appendix A). The Au/Ca ratio (Figure 18A) in the example below normalises Au by Ca, while the PolyMetal2 index adds the CLR values for Au, Cu, Ag, Mo, Pb and Zn for each sample (Figure 18B).

Table 4: Regolith ratios calculated via the Next Gen Analytics workflow from multi-element geochemical as well as spectral analyses of ultrafine soil samples. Non CLR data = uses the elemental concentrations, e.g., ppm or instrument reported values.

Regolith Ratio	Calculation	Comments
Au/Ca	Au divided by Ca	Non CLR data
Au/Fe	Au divided by Fe	Non CLR data
Au/FePhase	Au divided by Hem:Goeth	Non CLR data; FePhase relates to VNIR data; where FePhase is not detected there is no value and the ratio will not be calculated
Au/OrgC	Au divided by Organic Carbon	Non CLR data; relates to FTIR data; where TOC is not detected there is no value and the ratio will not be calculated
Au/SSA	Au divided by Specific Surface Area	Non CLR data; relates to sizing data
Au/Mn	Au divided by Mn	Non CLR data
Ca/Mg	Ca divided by Mg	Non CLR data
Pt/Pd	Pt divided by Pd	Non CLR data
Rb/Sr	Rb divided by Sr	Non CLR data
Th/U	Th divided by U	Non CLR data
Ti/Zr	Ti divided by Zr	Non CLR data
Zr/Sc	Zr divided by Sc	Non CLR data

Table 5: Exploration indices calculated via the Next Gen Analytics workflow from multi-element geochemical analyses of ultrafine soil samples. CLR = Centred Log Ratio (compositional data transformation addressing issues with closure, presenting numerically simpler values which are potentially easier to work with).

Exploration Indices	Calculation	Comments*
CHI6	As+Sb+Bi+Mo+Ag+Sn+W+Se	Addition of CLR values
Gold1	Au+Ag+As+W+Sb+Bi	Addition of CLR values
Gold2	Au+As+Bi+Te+S	Addition of CLR values
Gold3	Au+As+Sb	Addition of CLR values
Greenstone	Cr+V-U	Addition and subtraction of CLR values
IOCG	Cu+U+Au+Sm+Ce+La+Y+Sc	Addition of CLR values
IOCG+Br	Above + Br	Addition of CLR values; only if Br analysed
Komatiite	Ni-Cr	Subtraction of CLR values
NiPGE	Ni+Pt+Cu+Co+As+Te	Addition of CLR values
NiPGE+Pd	Above + Pd	Addition of CLR values; only if Pd analysed
PEG4	As+Sb+Sn+Nb+Ta	Addition of CLR values
Pegmatite1	Li+Ta+Cs+Nb	Addition of CLR values
PolyMetal1	Ag+Au+As+Sb+Mn+Ba+Te	Addition of CLR values
PolyMetal2	Au+Cu+Ag+Mo+Pb+Zn	Addition of CLR values
PorphyryD	Tl+Li+Sb	Addition of CLR values
PorphyryL	Mo+Cu+Ca-As-Mn-Zn-Co-K	Addition and subtraction of CLR values
PorphyryP	Bi+Te+Mo+Sn+Cu+W+Se	Addition of CLR values
REE4	Ce+La+Y+Sc	Addition of CLR values
SedCu	Cu+Zn+Pb+Bi+Co+Ni+As+Ag+Au	Addition of CLR values
SnWGran	Sn+W+Mo	Addition of CLR values
SnWGran+I	Above + I	Addition of CLR values; only if I analysed
VMS_MVT	Ag+Pb+Zn+Cd+Cu+Tl	Addition of CLR values

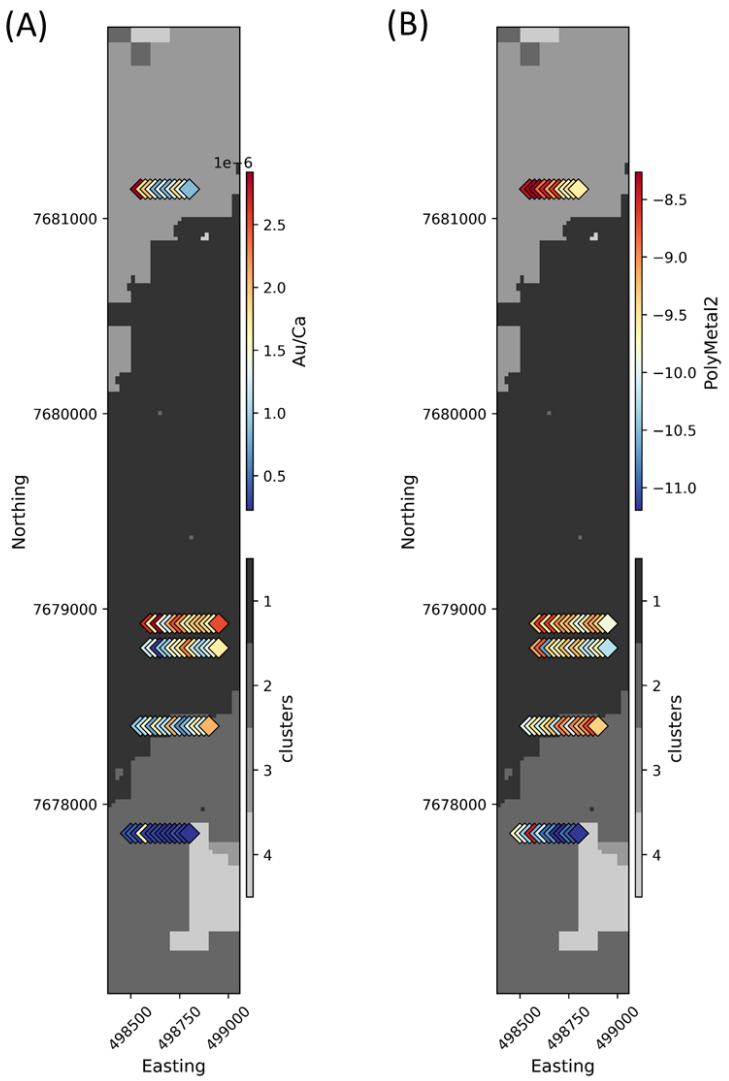

Figure 18: Example of maps of regolith ratios and indices generated from UltraFine+® data as an automated output of the Next Gen Analytics workflow. (A) Spatial distribution of Au divided by Ca. (B) Spatial distribution of the PolyMetal2 index generated by adding CLR values of Au, Cu, Ag, Mo, Pb and Zn.

3.5 Other Soil Properties

In addition to the multi-element geochemistry suite, several other soil parameters that are related to understanding metal mobility have been added to the UltraFine+® Next Gen Analytics workflow. These include pH, conductivity, particle size distribution, and visible to near-infrared (VNIR) mineral proxies and mid-infrared spectral properties (using a Fourier transform infrared (FTIR) spectroscopy). This data is intended to be used for the identification of soil property trends to enable the interpretation of geochemical results within landscape context, especially with respect to better explaining false positive results. At the time of analysing the Jericho samples, much of the methods for testing for these additional soil properties were still under development and since then methods of data acquisition, processing and QA/QC have been refined. In addition, larger scale data comparison between different project sites to identify broader trends is ongoing. It is important to note that soil sample density in the project area is very sparse and does not extend into areas that are likely representative of background concentrations. This limits the ability for data interpretation in a surface exploration context.

3.5.1 Soil pH and electrical conductivity (EC)

The mobility (solubility, transport and precipitation) of many metals, such as the elements of interest in the Jericho project area, are driven by pH and redox state. The pH of soils is mainly dependent on the mineralogy of the parent material and is, for example, expected to be more acidic around sulphide-rich deposits and more alkaline where parent material has higher buffering capacity, e.g., via silicate- or carbonate-mediated buffering during weathering and soil formation. Soil pH can, therefore, be a useful indicator for broad lithological changes, and potentially indicate certain types of mineral occurrences. Hence, it can be a useful tool to confirm landscape types for better context during geochemical sample interpretation. The EC indicates the salinity of soils, which in turn can affect the mobility of metals, such as Cu, Pb and Zn (Acosta et al. 2011).

Soil pH within the Jericho project area is slightly acidic to alkaline, ranging from pH 5.0 to pH 9.4 with an average circumneutral pH of 6.9 (Figure 19A, C). Soil EC over the Jericho project area is generally very low (<175 µS/cm) indicating non-saline soils with an average soil EC of 29.5 µS/cm and only one isolated value of >175 µS/cm (Figure 19B).

Within the Jericho project area, pH appears to be strongly associated with landscape clusters. The sand plain material in the south of the project area (orange landscape cluster 2) is generally more alkaline (average pH of 7.8; Figure 19C), while pH in the dark red-brown landscape cluster 1 (ferricrete soil) is more acidic (pH ≈6.6). Soils in sand plain 2 to the north of the project area (light-blue landscape cluster 3) are the most acidic (Figure 19C). The more alkaline sheetwash soils (orange landscape cluster 2) in the south of the project area generally display lower concentrations for elements such as Au and Cu (Figure 12B-C). However, there is insufficient data over this project site to establish causal relationships.

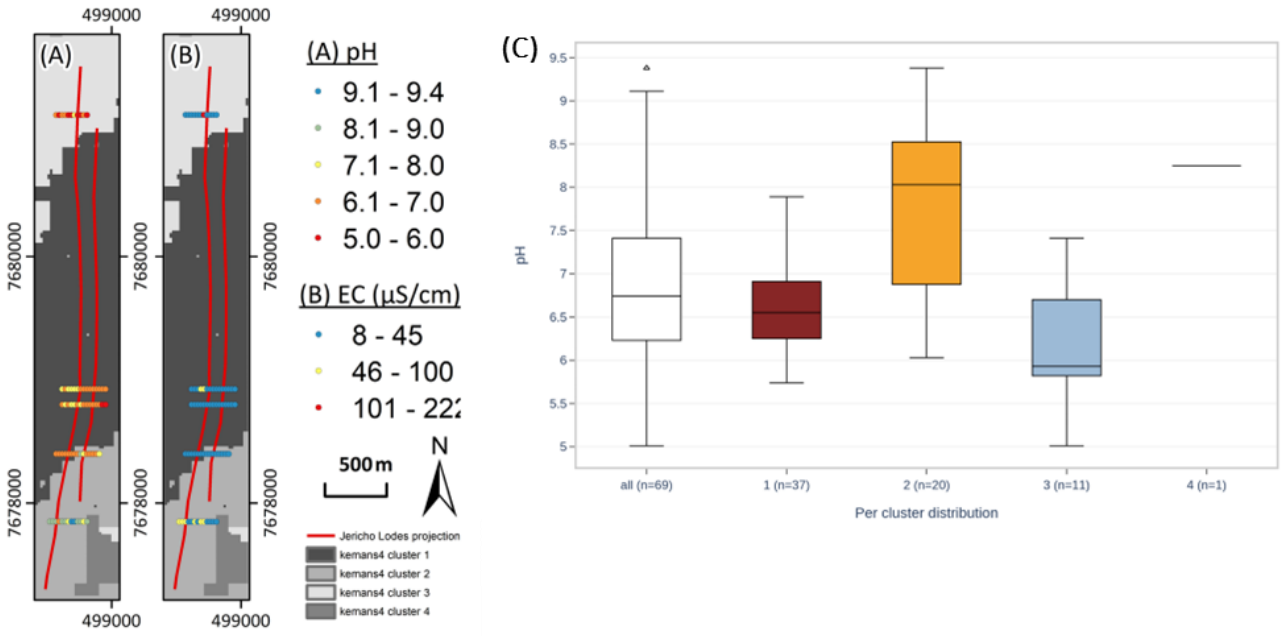

Figure 19: Spatial distribution of soil pH and EC over the Jericho project area. (A) pH. (B) EC in µS/cm. (C) Boxplots for all pH data (white box) and by landscape type (coloured boxes) when calculated based on four landscape clusters.

3.5.2 Soil sizing and texture

Due to their affinity to the clay fraction, the mobility of many metals in soil is linked to soil texture. The clay fraction effectively immobilises these metals, while a higher percentage of sand fractions with low binding strength leads to higher metal mobility (Rieuwerts et al. 1998). While the UltraFine+® soil sample analysis method takes this into account on an individual sample scale and especially within a specific landscape type, by extracting only the clay fraction of a given sample, the overall soil morphological environment will indicate larger scale soil development and composition. This in turn affects general trends of metal mobility in a given landscape environment and can inform the context for the machine learning derived landscape clusters and the geochemical assay results.

The UltraFine+® method reports particle size analysis as a standard output, with the percentage of sand, silt, and clay in bulk (<2 mm) soil samples. These values are used in the Next Gen Analytics workflow to derive broad soil textural classes and can be used to identify key changes in landscape soil morphology. The soil texture over the Jericho project area is sandy loam to silty-loam with little landscape variation with the exception of soil samples along the southernmost sample transect which indicate coarser materials corresponding to a change from ferricrete soils to sand plain and alluvial floodplain materials (compare Figure 20A with Figure 3A and Figure 8).

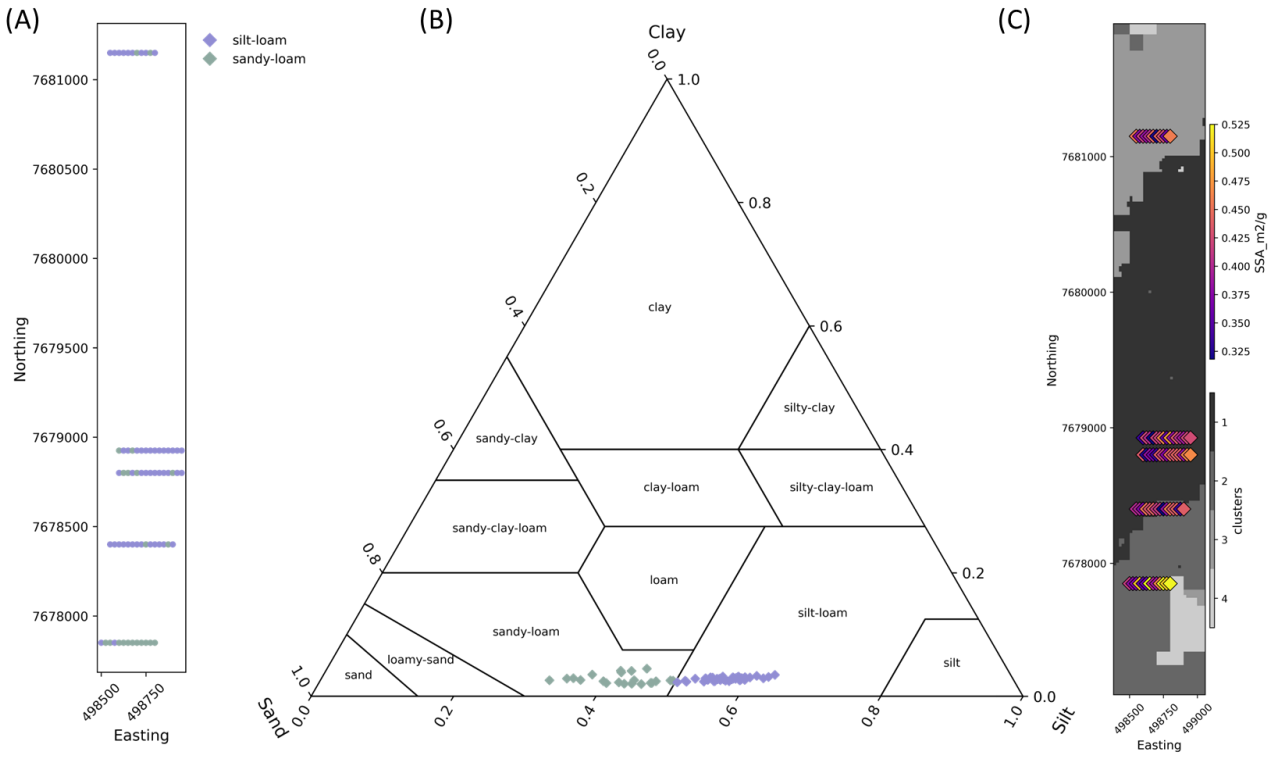

Figure 20: Next Gen Analytics workflow outputs generated from particle size distribution analyses of samples in the Jericho project area. (A) Spatial distribution of soil texture. (B) Soil texture diagram. (C) Spatial distribution of soil surface area.

In addition to the above, the UltraFine+® particle size analysis also measures the specific surface area of a given soil sample, which is an important control on cation exchange and adsorption capacity in soils (Macht et al. 2011) with surface area inversely related to the particle size.

Similarly to the soil texture, a difference in specific surface area was reported for some samples along the southernmost sample transect (Figure 20C). Owing to the scarcity of the data, this spatial trend could be entirely accidental and no relationships to other analyses parameters (except for the obvious clay content) was identified, and specific surface area and soil texture in this project area is likely to have little influence on the observed variations in metal concentrations along the five sample transects.

3.5.3 Visible near-infrared spectroscopy (VNIR)

In addition to pH and EC, the concentration of many metals in soil samples is also related to the composition of a given sample, such as the abundance of iron oxides or clay phases. Visible to shortwave infrared reflectance measurements can indicate the presence of key spectrally active mineral groups and their chemistry, and provide relative abundance estimates for iron oxides and kaolinite. As of November 2022, 17 spectral soil parameters are reported with the UltraFine+® soil analysis, including main mineral groups detected in the visible to shortwave infrared region. The main mineral groups (Mineral Group 1 and 2) report only the dominant mineral-group that contributes >51 % to the spectral unmixing algorithm and does not report individual minerals but mineral groups (e.g., white mica rather than muscovite). The mineral groups reported with the UltraFine+® method are Kaolin, Smectite, White-Mica, Amphibole, Chlorite, Dark-Mica, Al-bearing minerals, Mg-bearing minerals, Carbonate and Sulphate.

While some trends can be observed, data points for the Jericho project area are very limited. It is also important to note that larger scale data comparisons between different project sites to identify broader trends across multiple datasets from locations on the Australian continent was ongoing at the time of writing this report.

Figure 21 (next page): Spatial distribution of spectrally active mineral groups and other VNIR parameters in ultrafine soil samples over the Jericho project area. (A) Mineral group 1. (B) Mineral group 2. “Nomatch” refers to minerals that have no match in the current library. (C) Relative iron oxide abundance. (D) Iron oxide species. Lower values (dark red) indicate more hematitic materials, whereas higher values (yellow-brown) indicate that the material is more goethitic. Note that where Fe-oxide abundance is very low, the iron oxide species is not identified, and data is not plotted. (E) Relative kaolinite abundance. (F) Relative kaolinite crystallinity. (G) Saturation which indicates how washed out or pure the hue of a colour is. Current resource model area is indicated in yellow.

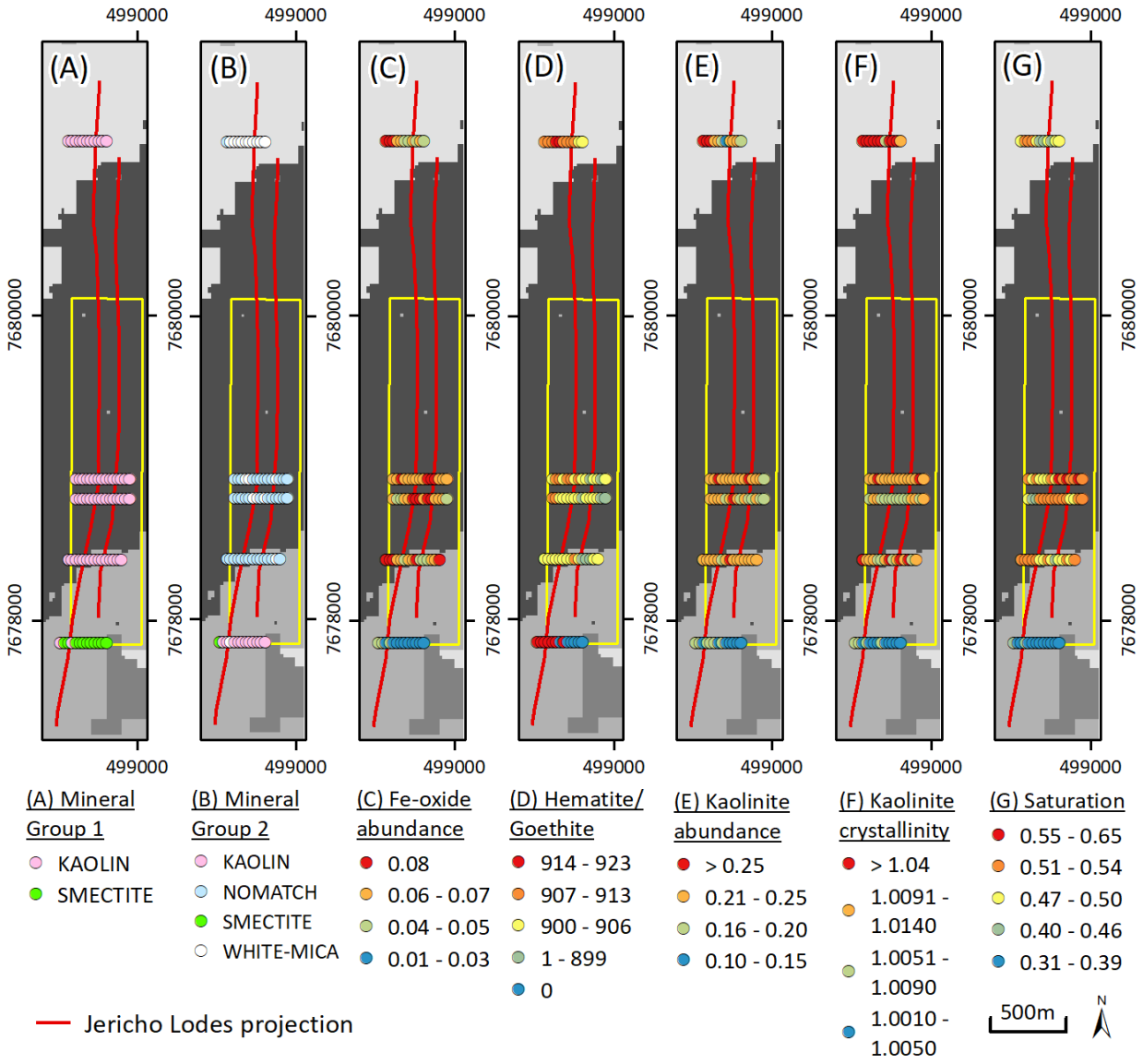

The analysed soil samples in the Jericho project area are dominated by kaolinite as the main clay mineral group, with smectite only detected in sand plain materials in the south of the project area (orange landscape cluster 2; Figure 21A). More distinct differences between landscape types become apparent in the secondary clay mineralogy, where white mica is identified in sand plain material in the north of the project area (light blue landscape cluster 3; Figure 21B), while kaolinite is prevalent as the secondary mineral group in the sheetwash material in the south (orange landscape cluster 2). The ferricrete soil (dark brown landscape cluster 1; Figure 21B) is dominated by a mineral(s) that cannot be identified by the current unmixing algorithms and minor white mica. Despite the scarcity of the samples across the project area, the observed changes in clay mineralogy broadly reflect the different landscape types (Figure 21). While both landscape cluster 2 (orange) and 3 (light blue) can be loosely defined as sand plain, there are mineralogical differences likely related to parent materials and weathering processes. Smectite group minerals, which are indicated in sand plain 1 (south, orange landscape cluster 2) are common during weathering close to mafic rocks (nontronite/saponite) or in alluvial settings (montmorillonite), and indeed this landscape cluster is proximal to a broader alluvial channel (dark blue landscape cluster

4). White mica, indicated in sand plain 2 (north, light blue landscape cluster 3) is commonly found associated with shallow soils near, or adjacent to, granitic material.

Other spectral properties follow similar trends to the main mineral groups, effectively differentiating different landscape types. Unsurprisingly, relative abundance of iron oxides is moderately high within the ferricrete soil dominated project area, except for the more alluvial materials in the south (Figure 21C). Soils in these landscape settings (orange landscape cluster 2 and dark blue landscape cluster 4) are notably more goethitic rather than hematitic or bear little to no iron oxides (Figure 21D). Relative kaolinite crystallinity follows a similar trend (Figure 21E). Values below 1.015 are traditionally considered disordered and the kaolinite crystallinity of most soil samples within the Jericho project area are poorly to moderately ordered. However, these values were derived on different sample materials (rock chips) and the presence of smectite in soil samples can reduce the numerical value of the kaolinite crystallinity. Therefore, separating traditional levels of confidence for kaolinite crystallinity (>1.05 = high, 1.05 to 1.015 = moderate, <1.015 = disordered) might not be appropriate for this data and we have adjusted these values slightly for soil interpretation (see legend in Figure 21F). Hence, we focus here on subtle variations in the data that correspond to landscape clusters and, in the case of the Jericho project area we can distinguish the more alluvial landscape types (orange landscape cluster 2 and dark blue landscape cluster 4) as containing little kaolinite with very low crystallinity, indicating transported cover. Soil colour is another interesting property measured from the spectra, since it is related to soil composition. It is not surprising that the Munsell® colour of samples often follows general landscape cluster boundaries. One component of the soil colour, the saturation, within the Jericho project area correlates spatially well with the trends observed above (Figure 21G).

While the above examples are mainly qualitative in nature, and are intended to supplement the interrogation of anomalies, some parameters may be used to normalise geochemical data. This includes swelling vs. non-swelling clays (e.g., kaolinite vs. smectite) as well as the relative iron-oxide abundance. Many trace metals are readily adsorbed to clays and iron oxides, especially those with a high surface area. Given the high adsorption capacity of iron oxides, it is often worth considering whether an anomaly of a metal of interest is present in iron oxide-rich or -poor soils and normalise the geochemical data accordingly. Although the cover at Jericho is likely too deep for detection of geochemical anomalies by surface exploration techniques and the sample transects do not extend into background chemistry, we demonstrate here an example of how the VNIR data could be used to normalise metals of interest, Ag, Au and Cu (Figure 22A, C, E) with relative iron oxide abundance (Figure 22B, D, F). On a relative scale this exercise downgrades higher metal values in iron-rich soils while it upgrades those in iron-poor soils (e.g., compare sample transect 5 across Figure 22A to F).

Figure 22 (next page): Example of normalising geochemical data with VNIR analyses. (A) Spatial distribution of Ag abundance in ppm. (B) Spatial distribution of Ag normalised to relative iron oxide abundance. (C) Spatial distribution of Au concentrations in ppb. (D) Spatial distribution of Au normalised to relative iron oxide abundance. (E) Spatial distribution of Cu concentrations in ppm. (F) Spatial distribution of Cu normalised to relative iron oxide abundance.

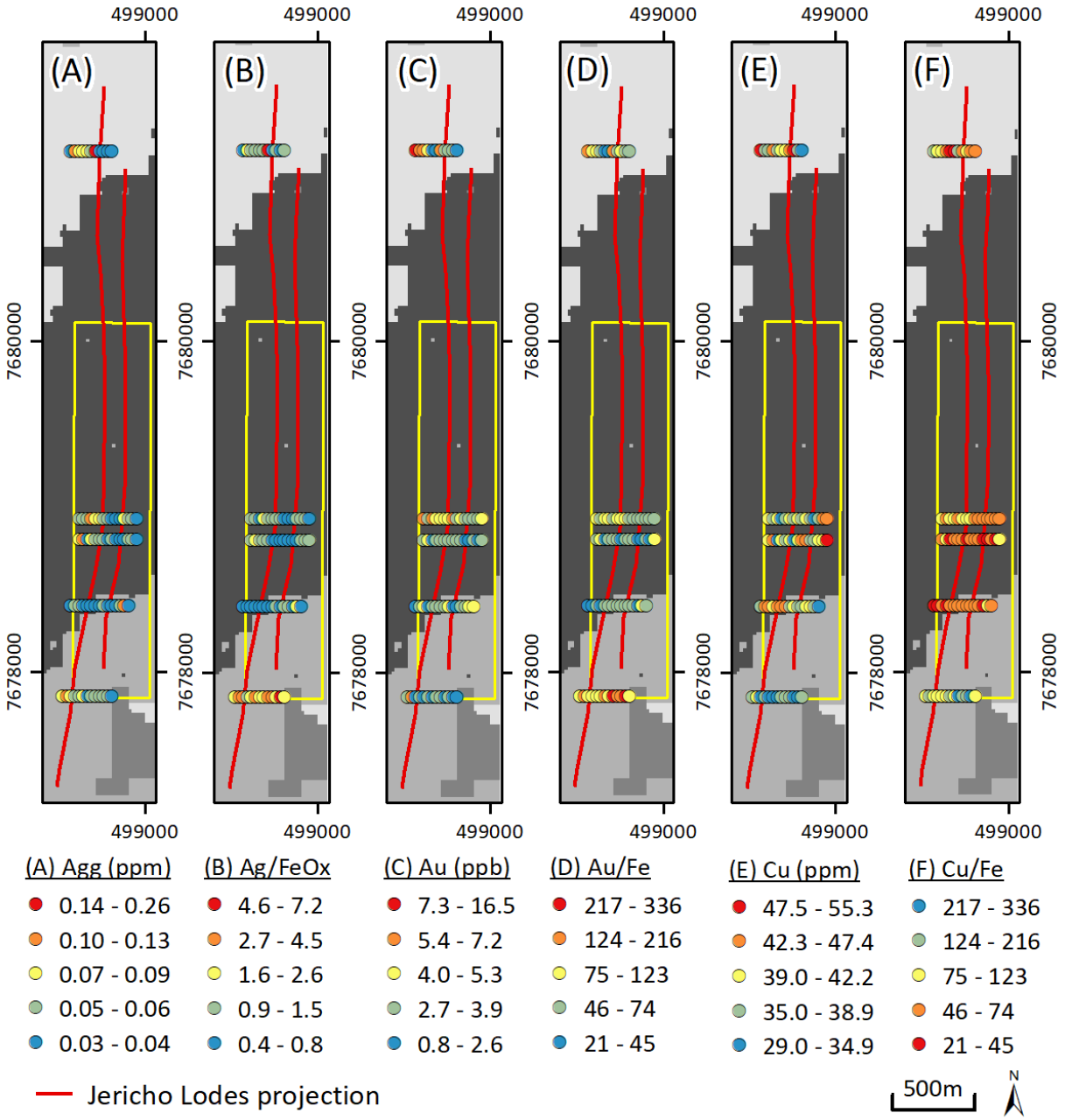

3.6 Dispersion and source direction

Both source direction and dispersion direction are generated from the UltraFine+® Next Gen workflow and are available as shapefiles and as toggles in the Digital Sample Observer (see section 3.7). The source direction is derived for each sample with the arrow pointing up-slope and proportional to the steepness (likely greater dispersion distance). It is important to note that the accuracy of the source direction depends on the accuracy of the GPS reading of a given soil sample and multiple adjacent sample points should be considered when interpreting the likely source direction of a geochemical anomaly in transported cover.

The dispersion direction is calculated on a grid over each project area rather than on each sample point and the arrows point down-slope and are intended to give a first-glance overview of broader dispersion trends within an area. This can be a useful tool for larger survey areas with transported cover and potential for infill sampling.

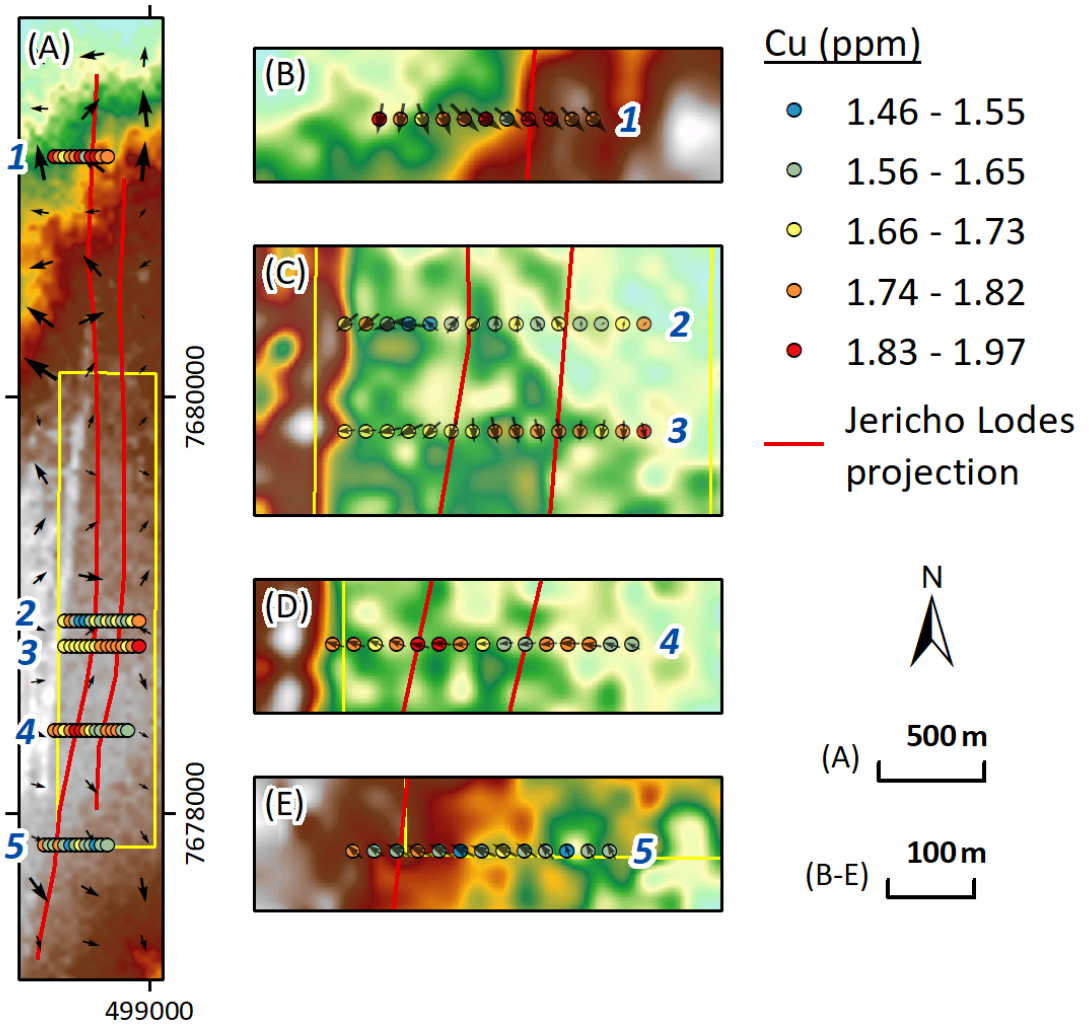

Figure 23: Source and dispersion direction over the Jericho project area. (A) Dispersion direction grid and Cu concentrations in soil along the 5 sample transects across the Jericho lodes. Dispersion directions indicate broad scale trends. Arrows and numbers are proportional to the slope degree. (B - E) Source direction of individual soil sample points and Cu concentrations along sample transects 1 (B), 2 and 3 (C), 4 (D) and 5 (E). Source direction is calculated from the DEM (background) but is dependent on accurate GPS readings of each soil sample.

The basement rocks in the Jericho project area are truncated by an unconformity, overlain by sedimentary units which in turn have been covered by transported sediments. However, dispersion and source direction only take current slope directions into account and palaeo-relief is not considered. Even if there was a dispersal mechanism from ore at depth to the surface (e.g., along the shear zone) the slope within the area is a maximum of 1 degree. While surface dispersion can have a significant effect over time and space even in such flat landscape settings, a larger-scale survey would need to be considered.

3.7 The Digital Sample Observer (DSO)

The UltraFine+® and Next Gen Analytics workflow produces a wealth of data and integrates geochemical information with landscape settings. While this provides the explorer with a variety of first-pass interpretation tools, exploration in (transported) cover and the plethora of additional data is not easily visualised and interrogated all at once. The Digital Sample Observer (DSO; Figure 24) was developed as a user-friendly tool for easy visualisation and first-pass interrogation.

Generally, the DSO is provided as an Overview DSO (with all landscape models and input layers) as well as a DSO for each model. The DSO allows for UltraFine+® analyses and Next Gen Analytics workflow outputs to be toggled on and off in spatial context. This is best explored live (you can access the DSO for the Jericho project area in Appendix A).

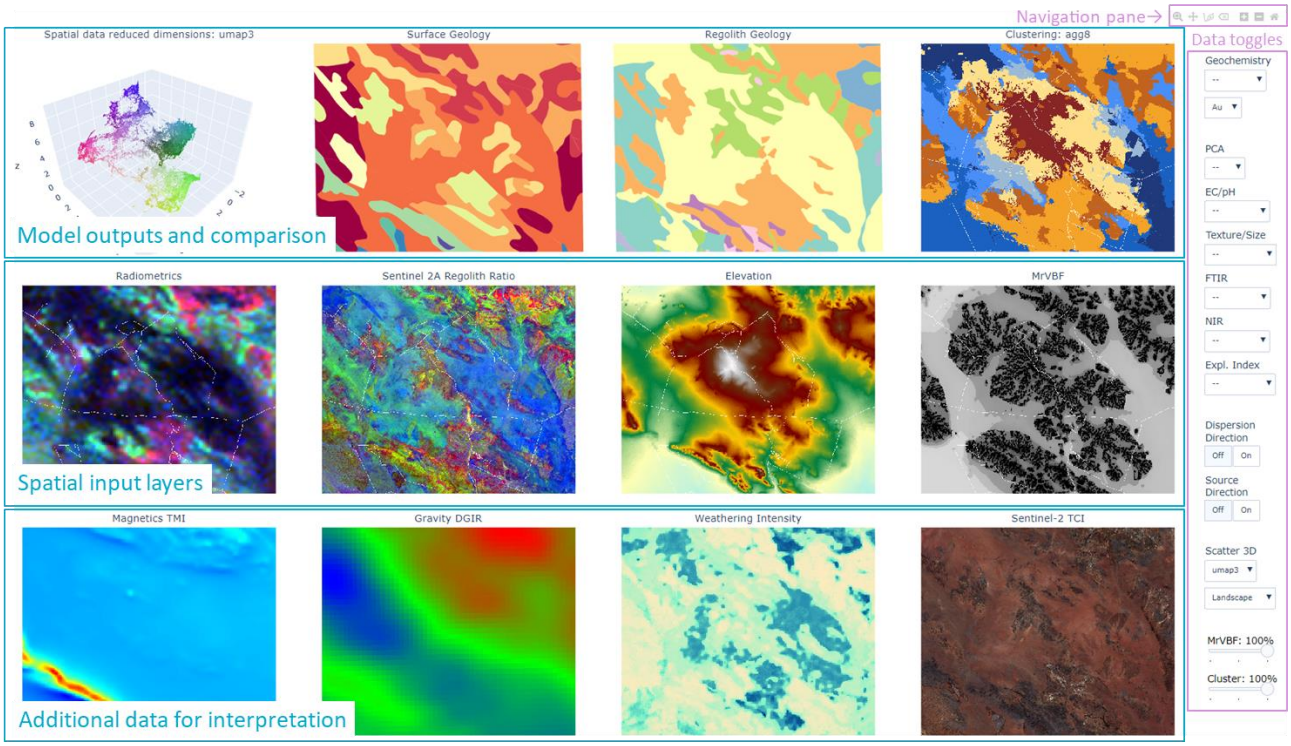

Figure 24: Overview of the html-based DSO for a landscape model with 8 clusters over a large de-identified survey area with over 5000 samples. All data available for these soil samples can be toggled on and off.

4 Summary

This report demonstrated some of the outputs of the UltraFine+® Next Gen Analytics workflow with the goal of using machine learning to integrate spatial data features to provide landscape context for geochemical data and basic, first-pass data interpretation. The UltraFine+® Next Gen Analytics workflow used machine learning to integrate spatial data and soil properties in several derived outputs which included proxy regolith landscape clusters, maps and boxplots of elemental outliers by landscape type, principal component analysis, exploration indices, soil texture diagrams, soil property maps for VNIR data, and dispersion and source direction. Most of these outputs are available in GeoTIFF, PNG, shapefile and CSV formats. Some components of the UltraFine+® method (e.g., mid-infrared spectral properties) were still under development during data acquisition and were therefore not available for the Jericho project site.

The Geological Survey of Queensland provided 69 “blind” soil samples in 2019 over the Jericho deposit in QLD to support the UltraFine+® Next Gen Analytics research project. These samples were collected by Minotaur Resources Ltd who held the tenement over the Jericho Cu deposit at the time. The tenement has since changed ownership to Demetallica Ltd and currently to AIC Mines Ltd.

The ore at Jericho is hosted in two shears in Proterozoic basement rocks that are truncated by an unconformity overlain by Mesozoic mudstone which in turn is covered by thick transported Tertiary and Quaternary fluvial sediments. Given the thickness of sedimentary cover, the depth of mineralised intercepts in basement rocks (several hundred metres) and little-preserved weathering near the unconformity, it is unlikely for any soil geochemical sampling to identify element dispersion related to the mineralisation at depth. In addition, sample transects were located within the current resource polygon across the two lodes and did not extend into geochemical background. UltraFine+® results are therefore inconclusive and most observed geochemical trends could be entirely coincidental. Nevertheless, the Jericho soil samples, along with soil samples from other early supporters of the project, were crucial in refining the UltraFine+® method. The soil analytical method has undergone continuous improvements over the course of the research project (conducted from April 2020 to April 2023) which is reflected in improved detection limits and refined outputs. Since the data acquisition for the Jericho project site (August 2019), detection limits for 30 elements, including Cu and Ag, were improved. In addition, three elements, Pd, I and Br, were added to the multi-element suite and FTIR analysis was introduced to the workflow. VNIR data processing has also been refined and data presented herein was reprocessed with the latest TSG™ VNIR processing version in January 2023.

The Next Gen Analytics workflow was designed primarily for greenfields exploration in areas of shallow (<30 m) transported cover with hundreds to thousands of samples, and to generate interpretation of these soil samples prior to significant ground disturbance caused by major roads, built-up areas, and mining and agricultural infrastructure, as these can influence the spatial data input layers. While the small number of samples and ground disturbance over the Jericho project area limit the value of interpreting samples by landscape type for this specific site, the project area provided a valuable example site to test the workflow over known mineralisation for a suite of

elements in deep cover. Multiple iterations of the workflow have been run over the Jericho area during the developmental phase of the research project and in this report, we present outputs that were re-processed in November 2022 upon finalisation of the Next Gen Analytics workflow. While the available data and the scale of the project site were limited, the focus for this project site was on principal functionality and application of landscape recognition via machine learning in a known exploration setting and testing its limitations.

We demonstrated two landscape models with four and eight clusters which represent proxy regolith types of the project area. Both outputs provided more landscape context than publicly available surface geology and regolith maps. However, due to the small size of the project area, kmeans4 is the preferred output that represents the main regolith features, although additional landscape classes provide details on secondary features, such as parent materials.

Some elevated concentrations appeared to coincide with the steeply west dipping Jericho lodes, with maximum concentrations of Ag at 0.26 ppm, Au at 16.5 ppb and Cu at 55.3 ppm against median values of 0.05 ppm Ag, 3.3 ppb Au, and 38.7 ppm Cu, and no sample was below the detection limit. However, there was a lack of data to identify the lateral background soil concentrations and/or information on dispersion mechanisms from depth to surface. Hence, these subtle elevated concentrations are likely to be entirely coincidental. Overall, the interpretation within landscape context over the Jericho project site was limited by the depth to mineralisation (>200 m), the small size of the area with exclusively depositional landscape settings, as well as the number of samples per landscape cluster. Hence, it was recommended to interpret these samples as a whole dataset rather than by landscape type. Individual outliers not apparent from the whole-population analyses were identified by landscape types for exploration-relevant elements such as Cd, Co, Cr, Mo, Pb, Sb and W, but these did not show relevant patterns.

With the limited samples and context available, principal component analysis, regolith ratios and indices, as well as other soil property analyses reflected landscape variety within the dataset rather than relevant exploration targets. This was especially apparent along sample transect 5, where the main principal component was positively loaded with Ca, Mg, Ba and Sr, reflecting the general change in soils at the southern edge of the project area, indicating carbonaceous regolith materials. This was confirmed by soil pH, which appeared to be strongly associated with landscape clusters and was slightly acidic to alkaline, ranging from pH 5.0 to pH 9.4 with an average circumneutral pH of 6.9. The more carbonaceous sand plain material in the south of the project area was generally more alkaline, while pH in ferricrete soil and the sand plain soil in the north of the project area was more acidic. Despite the scarcity of samples across the project area, other soil properties also reflected the different landscape types. Soil texture, which ranged from sandy loam to silty loam, followed this pattern, and mineral groups in VNIR data showed mineralogical differences likely related to parent materials and weathering processes. These were useful in differentiating the two sand plain materials in the north and south of the project site. Smectite group minerals (common during weathering close to mafic rocks (nontronite/saponite) or in alluvial settings (montmorillonite) only occurred in the south of the project area, while white mica was detected in the north of the project area and is commonly found associated with shallow soils near, or adjacent to, granitic material. Other spectral properties followed similar trends to the main mineral groups, effectively differentiating different landscape types.

To demonstrate an example of the machine learned landscape clustering approach for future greenfields exploration surveys in Queensland, we generated a larger area landscape proxy map (approximately 1,600 km^2) centred around the Jericho project area and the Eloise deposit with twelve landscape clusters. This landscape proxy map provides a much more in-depth landscape context than publicly available maps and can aid sample survey planning as well as data interpretation. Although the cover at Jericho is likely too deep for detection of geochemical anomalies by surface exploration techniques, and the sample transects do not extend far enough laterally to determine background chemistry, the Jericho study site was crucial in the refinement of the UltraFine+® soil analytical method in the early stages of the research project.

References

Acosta, J.A., Jansen, B., Kalbitz, K., Faz, A., Martínez-Martínez, S., 2011. Salinity increases mobility of heavy metals in soils. Chemosphere. 85(8):1318-24. doi: 10.1016/j.chemosphere.2011.07.046

Anand, R.R., Robertson, I.D.M., 2012. Role of mineralogy and geochemistry in forming anomalies on interfaces and in areas of deep basin cover-implications for exploration. Geochem.: Explor. Environ. Anal. 12, 45–66.

Anand, R., 2016. Regolith-landform processes and geochemical exploration for base metal deposits in regolith-dominated terrains of the Mt Isa region, northwest Queensland, Australia. Ore Geology Reviews, vol. 73, no. March 2016, pt. 3: 451-474.

Baker, T., 1994. The geology of the Eloise Copper-Gold deposit, NW Queensland, Australia. Proceedings of the Australasian Institute of Mining and Metallurgy Annual Conference. Darwin, pp. 109–204

Bureau of Meteorology, 2023. Online climate data for Cloncurry Mcillwraith station, http://www.bom.gov.au/climate/averages/tables/cw_029008.shtml [last accessed January 2023]

Demetallica 2022. https://demetallica.com.au/wp-content/uploads/2022/10/DRM_Jericho_Resource_Expanded_25-Oct-2022.pdf

Department of Resources, 2018. Detailed surface geology - Queensland [Digital dataset]. Department of Resources, Queensland. https://qldspatial.information.qld.gov.au/catalogue/custom/detail.page?fid={9BA2F66C-1933-4439-B9C9-E631911ADD7E}

Geoscience Australia, 2013. Regolith Map of Australia Edition 1- Digital. Geoscience Australia, Canberra. http://pid.geoscience.gov.au/dataset/ga/76662

Gallant, J., Austin, J., 2012a. Slope derived from 1" SRTM DEM-S. v4. CSIRO. Data Collection. https://doi.org/10.4225/08/5689DA774564A

Gallant, J., Austin, J., 2012b. Aspect derived from 1" SRTM DEM-S. v6. CSIRO. Data Collection. https://doi.org/10.4225/08/56D778315A62B

Gallant, J., Dowling, T., Austin, J., 2012. Multi-resolution Valley Bottom Flatness (MrVBF). v3. CSIRO. Data Collection. https://doi.org/10.4225/08/5701C885AB4FE

Gallant, J., Wilson, N., Dowling, T., Read, A., Inskeep, C., 2011. SRTM-derived 1 Second Digital Elevation Models Version 1.0. Record 1. Geoscience Australia, Canberra. http://pid.geoscience.gov.au/dataset/ga/72759

Gozzard, J.R., 2005. Part 3: Regolith-landform mapping using remotely sensed imagery in IGES 2005 Workshop 1.3, Regolith mapping, workshop notes: Perth, Western Australia, IGES 2005, 73p.

Hall, G.E.M., 1998. Analytical perspective on trace element species of interest in exploration, Journal of Geochemical Exploration, 61 (1–3): 1-19. https://doi.org/10.1016/S0375-6742(97)00046-0

Henne, A., Noble, R.R.P., Huang, F., Cole, D., Williams, M., Ibrahimi, T., Lau, I.C., Pejcic, B., 2022. UltraFine+® Next Gen Analytics. Geological Survey of New South Wales – Cobar Projects. CSIRO Report EP2022-3306, CSIRO, Australia.

Isbell R.F., 2021. National Committee on Soil and Terrain. The Australian Soil Classification. 3rd edn. CSIRO Publishing, Melbourne.

Minotaur Exploration Limited, 2019. Jericho Copper-Gold Discovery: What Lurks Beneath the Deep Blue Sea; GSQ Technical Workshop 20-21 March 2019
https://smi.uq.edu.au/files/43680/1903_Isa_D1_08_Little_Jericho.pdf

Li Shu, Robertson, I.D.M., 1997. Surficial geology around the Eloise area and dispersion into Mesozoic cover from the Eloise mineralisation. CRC LEME Restricted Report 56R (71 pp. (Reissued as Open File Report 135, CRC LEME, Perth, 2002)).

Macht, F., Eusterhues, K., Pronk, G.J., Totsche, K.U., 2011. Specific surface area of clay minerals: Comparison between atomic force microscopy measurements and bulk-gas (N2) and -liquid (EGME) adsorption methods, Applied Clay Science, 53 (1): 20-26. https://doi.org/10.1016/j.clay.2011.04.006.

MacQueen, L., 1967. Some methods for classification and analysis of multivariate observations, in: Le Cam, L.M., Neyman, J. (Eds.), Berkeley Symposium on Mathematical Statistics and Probability. University of California, pp. 281–297. https://projecteuclid.org/proceedings/berkeley-symposium-on-mathematical-statistics-andprobability/proceedings-of-the-fifth-berkeley-symposium-on-mathematical-statisticsand/Chapter/Some-methods-for-classification-and-analysis-of-multivariateobservations/bsmsp/1200512992?tab=ChapterArticleLink

McInnes, L., Healy, J., Melville, J., 2018. "Uniform manifold approximation and projection for dimension reduction". arXiv:1802.03426

Noble, R., Lau, I., Anand, R., Pinchand, T., 2018. MRIWA Report No. 462: Multi-scaled near surface exploration using ultrafine soils: Geological Survey of Western Australia, Report 190, 99p.

Noble, R.R.P., Lau, I.C., Anand, R.R. and Pinchand, G.T., 2020. Refining fine fraction soil extraction methods and analysis for mineral exploration. Geochemistry; Exploration, Environment, Analysis 20(1):113-128. https://doi.org/10.1144/geochem2019-008

Pedregosa, F., Varoquaux, G., Gramfort, A., Michel, V., Thirion, B., Grisel, O., Blondel, M., Prettenhofer, P., Weiss, R., Dubourg, V., Vanderplas, J., Passos, A., Cournapeau, D., Brucher, M., Perrot, M., Duchesnay, É., 2011. Scikit-learn: Machine Learning in Python. *The Journal of Machine Learning Research*, *12*(null), 2825–2830.

Poudjom Djomani, Y., Minty, B.R.S., 2019c. Radiometric Grid of Australia (Radmap) v4 2019 filtered ppm uranium. Geoscience Australia, Canberra. http://dx.doi.org/10.26186/5dd48ee78c980

Poudjom Djomani, Y., Minty, B.R.S., 2019a. Radiometric Grid of Australia (Radmap) v4 2019 filtered pct potassium grid. Geoscience Australia, Canberra. http://dx.doi.org/10.26186/5dd48d628f4f6

Poudjom Djomani, Y., Minty, B.R.S., 2019b. Radiometric Grid of Australia (Radmap) v4 2019 filtered ppm thorium. Geoscience Australia, Canberra. http://dx.doi.org/10.26186/5dd48e3eb6367

Rieuwerts, J.S., Thornton, I., Farago, M.E., Ashmore, M.R., 1998. Factors influencing metal bioavailability in soils: preliminary investigations for the development of a critical loads approach for metals, Chemical Speciation & Bioavailability, 10:2, 61-75. DOI:10.3184/095422998782775835

Soil Science Division Staff, 2017. Soil Survey Manual. Eds. Ditzler, C., Scheffe, K., Monger, H.C., Government Printing Office.
https://www.nrcs.usda.gov/wps/portal/nrcs/detail/soils/ref/?cid=nrcs142p2_054262

Wilford, J., Roberts, D. 2019. Weathering Intensity Model of Australia. Geoscience Australia, Canberra. DOI:10.26186/5c6387a429914.

Williams, M. J., Schoneveld, L., Mao, Y., Klump, J., Gosses, J., Dalton, H., Bath, A., & Barnes, S. 2020. Pyrolite: Python for geochemistry. Journal of Open Source Software, 5(50), 2314.
https://doi.org/10.21105/joss.02314

Appendix A - UltraFine+® Next Gen Analytics data package – Jericho

Appendix B – Regional machine learning derived landscape model

As Australia's national science agency and innovation catalyst, CSIRO is solving the greatest challenges through innovative science and technology.

CSIRO. Unlocking a better future for everyone.

Contact us

1300 363 400
+61 3 9545 2176
csiroenquiries@csiro.au
csiro.au

For further information

Mineral Resources
Ryan Noble
+61 8 6436 8684
ryan.noble@csiro.au

Anicia Henne
+61 8 6438 8697
anicia.henne@csiro.au